Article

Identification of a Novel 1,2,3,4-tetrahydrobenzo[*b*][1,6]naphthyridine Analog as a Potent Phosphodiesterase 5 Inhibitor with Improved Aqueous Solubility for the Treatment of Alzheimer's Disease

Jole Fiorito, Jeremie Vendome, Faisal Saeed, Agnieszka Staniszewski, Hong Zhang, Shijun Yan, Shi-Xian Deng, Ottavio Arancio, and Donald W. Landry

J. Med. Chem., **Just Accepted Manuscript** • DOI: 10.1021/acs.jmedchem.7b00979 • Publication Date (Web): 06 Oct 2017

Identification of a Novel 1,2,3,4-tetrahydrobenzo[*b*][1,6]naphthyridine Analog as a Potent Phosphodiesterase 5 Inhibitor with Improved Aqueous Solubility for the Treatment of Alzheimer's Disease.

Jole Fiorito,[‡,#] *Jeremie Vendome,*[I,†,#] *Faisal Saeed,*[‡,†] *Agnieszka Staniszewski,*[‡] *Hong Zhang,*[‡] *Shijun Yan,*[‡,†] *Shi-Xian Deng,*[§] *Ottavio Arancio,*[‡,*] *Donald W. Landry*[§,*]

[‡]Taub Institute for Research of Alzheimer's Disease and the Aging Brain, Columbia University, 630 W 168th Street, New York, NY 10032.

[I]Department of Systems Biology, Columbia University Medical Center, New York, NY 10032.

[§]Department of Medicine, Columbia University, 650 W 168th Street, New York, NY 10032.

KEYWORDS. PDE5, PDE5 inhibitors, Alzheimer's disease, Naphthyridines, Long-term Potentiation, Learning, Memory, *In silico* Docking.

ABSTRACT

Phosphodiesterase 5 (PDE5) hydrolyzes cyclic guanosine monophosphate (cGMP) leading to increased levels of cAMP response element binding protein (CREB), a transcriptional factor involved with learning and memory processes. We previously reported potent quinoline-based PDE5 inhibitors (PDE5Is) for the treatment of Alzheimer's disease (AD). However, the low aqueous solubility rendered them undesirable drug candidates. Here we report a series of novel PDE5Is with two new scaffolds, 1,2,3,4-tetrahydrobenzo[*b*][1,6]naphthyridine and 2,3-dihydro-1*H*-pyrrolo[3,4-*b*]quinolin-1-one. Among them, compound **6c**, 2-acetyl-10-((3-chloro-4-methoxybenzyl)amino)-1,2,3,4-tetrahydrobenzo[*b*][1,6]naphthyridine-8-carbonitrile, the most potent compound, has excellent *in vitro* IC_{50} (0.056 nM) and improved aqueous solubility as well as good efficacy in a mouse model of AD. Furthermore, we are proposing two plausible binding modes obtained through *in silico* docking, which provide insights into the structural basis of the activity of the two series of compounds reported herein.

INTRODUCTION

Alzheimer's disease (AD) is the most common type of dementia and the sixth-leading cause of death in the United States. AD is a neurodegenerative disorder that compromises the ability of thinking, memory, and behavior. Senile plaques and neurofibrillary tangles, comprised of amyloid-beta (Aβ) peptide and microtubule binding protein tau, respectively, are the two main pathological hallmarks of AD. To date, no effective therapies have been developed for AD and only symptomatic treatments are available.[1,2] Therefore, major efforts are ongoing to find better ways to prevent the progression of this disease. Several biological pathways have been considered for developing valid therapeutic approaches, such as Aβ targeted strategies, tau-based

therapies, oxidative stress reduction, anti-inflammatory drugs, and therapies targeting second messenger systems that are impaired by either Aβ or tau.[1, 2] However, drugs that entered the clinical trials, e.g. most recently solanezumab, bapineuzumab, and aducanumab, which are humanized anti–Aβ monoclonal antibodies, have failed to improve clinical outcomes in patients or shown to induce adverse effects, e.g. vasogenic edema, making the Aβ-removing therapy a doubtful strategy to pursue for the treatment of AD.[3-5]

Here we have focused our attention on therapies targeting the nitric oxide (NO) signaling pathway because of its relevance to learning and memory processes.[6] Specifically, NO stimulates soluble guanylate cyclase (sGC), resulting in increased levels of second messenger cyclic guanosine monophosphate (cGMP) and activation of cGMP-dependent protein kinase (PKG), which is important for promoting the phosphorylation of cyclic adenosine monophosphate (cAMP) response element binding protein (CREB) at its Ser133.[7, 8] Phosphorylation of CREB has been recognized as a crucial event for gene transcription during synaptic plasticity, which is one of the fundamental processes underlying learning and memory.[9-11] Targeting the NO/cGMP/PKG/CREB signaling pathway can be achieved through the inhibition of phosphodiesterases (PDEs). PDEs are a superfamily of enzymes consisting of eleven subfamilies (PDE1-11) that hydrolyze the two nucleotides cGMP and cAMP into their inactive forms. One fundamental distinction between the subfamilies is based on their different affinity for the two substrates. PDE5, 6, and 9 are cGMP-specific enzymes, PDE4, 7, and 8 are cAMP-specific enzymes, while the remaining enzymes are dual-substrate PDEs, having affinity for both cyclic nucleotides.[12] This superfamily of enzymes have been studied as targets for the treatment of various diseases, including erectile dysfunction, pulmonary arterial hypertension, cancer, schizophrenia, and AD.[12-15]

Over the past years, we have been interested in elucidating the involvement of the NO/cGMP/PKG/CREB signaling pathway in AD;[16] we have demonstrated that the inhibition of PDE5, which specifically catalyzes the hydrolysis of cGMP therefore reducing PKG activity, leads to an improvement of learning and memory in mouse models of AD.[6, 17, 18] Previous research in our laboratories led to a novel series of quinoline inhibitors of PDE5 (PDE5Is) represented by compound **1** (Figure 1). Compound **1** is a potent and selective PDE5 inhibitor as determined by an *in vitro* enzymatic assay [IC_{50} (PDE5) = 0.270 nM, IC_{50} (PDE6) = 0.339 μM]. When dosed at 3 mg/kg, elevation of cGMP in the hippocampus of mice was observed. Moreover, compound **1** rescues learning and memory as shown by a pharmacological treatment of two different AD mouse models.[18] However, a turbidimetric (kinetic) solubility screening revealed that compound **1** has low water solubility (Table 2). This poor physicochemical property precluded the advancement of **1** into additional preclinical studies.

In the course of our drug discovery program we have also discovered other classes of heterocyclic PDE5Is, deriving from compound **1** and represented by scaffold A and B (Figure 1). The two scaffolds were designed by locking the rotatable bonds of the hydroxymethyl group of compound **1** into a ring. By rigidifying the conformation of the parent compound we sought to improve the potency and selectivity of the new molecules. We then decided to investigate these new chemical entities with the aim to find a suitable lead compound. Herein, we report the design and synthesis of 1,2,3,4-tetrahydrobenzo[*b*][1,6]naphthyridine (scaffold A) and 2,3-dihydro-1*H*-pyrrolo[3,4-*b*]quinolin-1-one (scaffold B) ligands and their enzymatic activity. Notably, we could identify a PDE5 inhibitor, compound **6c**, that displays enhanced potency, retained selectivity, and improved water solubility with respect to compound **1**, as well as *in vivo* pharmacological efficacy in the APP/PS1 double transgenic mice[19] that manifest aberrant

accumulation of human Aβ driven by mutations in $APP_{695}^{K670N/M671L}$ and $PS1^{M146L}$. Additionally, we identified two plausible binding modes in the same pocket using *in silico* docking, which provides insights into the structural basis of the activity of the new series of compounds reported here. The validation of one of these binding modes as well as its usage for further optimization of the herein reported compounds *via* a structure-based approach are to be pursued in a following study.

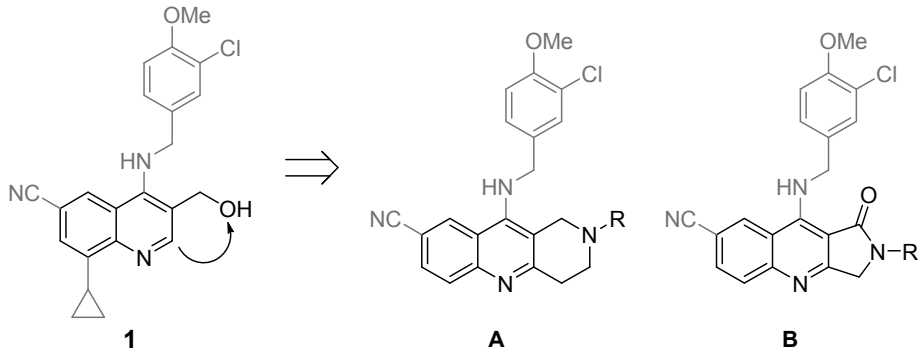

Figure 1. Structure of compound **1** and new PDE5Is: 1,2,3,4-tetrahydrobenzo[*b*][1,6]naphthyridine (scaffold A) and 2,3-dihydro-1*H*-pyrrolo[3,4-*b*]quinolin-1-one (scaffold B).

RESULTS AND DISCUSSION

Chemistry. As first step, we targeted the synthesis of a set of tricyclic analogs **6a-g** (scheme 1), **10** (scheme 2), and **13a-d** (scheme 3). As show in scheme 1, 2-amino-5-cyanobenzoic acid **4** was prepared via the cyanation of methyl bromobenzoate **2** with copper cyanide[22] followed by hydrolysis under basic conditions of ester **3**. For the synthesis of the 1,2,3,4-tetrahydrobenzo[*b*][1,6]naphthyridine core, a condensation reaction was used to synthesize intermediates **5a-d**.[23] Specifically, the reaction of **4** with the appropriate *N*-substituted piperidin-

4-one in $POCl_3$ gave **5a-d** in moderate yields (21-55%). Then, 3-chloro-4-methoxibenzylamine was introduced on the tricyclic ring of **5a-c** via nucleophilic substitution to obtain the final compound **6a-c**. Similarly, compounds **6d-f** were obtained by using the corresponding commercially available benzylamines (see Experimental Section for details). For the synthesis of compound **6g**, (3-chloro-5-fluoro-4-methoxyphenyl) methanamine hydrochloride **10** was prepared starting from the benzaldehyde **7**, which was initially reduced into benzyl alcohol **8** via a reduction reaction using $NaBH_4$. Subsequently, benzylamine **10** was obtained by following the Gabriel synthesis procedure (scheme 1). The synthetic route followed to prepare compound **14** was slightly different than the one used for synthesizing **6a-g** (scheme 2). Intermediate **5d** was first de-alkylated by using α-chloroethyl chloroformate (ACE-Cl); subsequently, after protecting the aliphatic nitrogen of **11** with a Boc group, the synthesis of **13** was accomplished via the same nucleophilic substitution reaction conditions used for compounds **6a-g**. Finally, removal of the Boc group gave the desired analog **14**.

Scheme 1. Synthesis of compounds 6a-g[a]

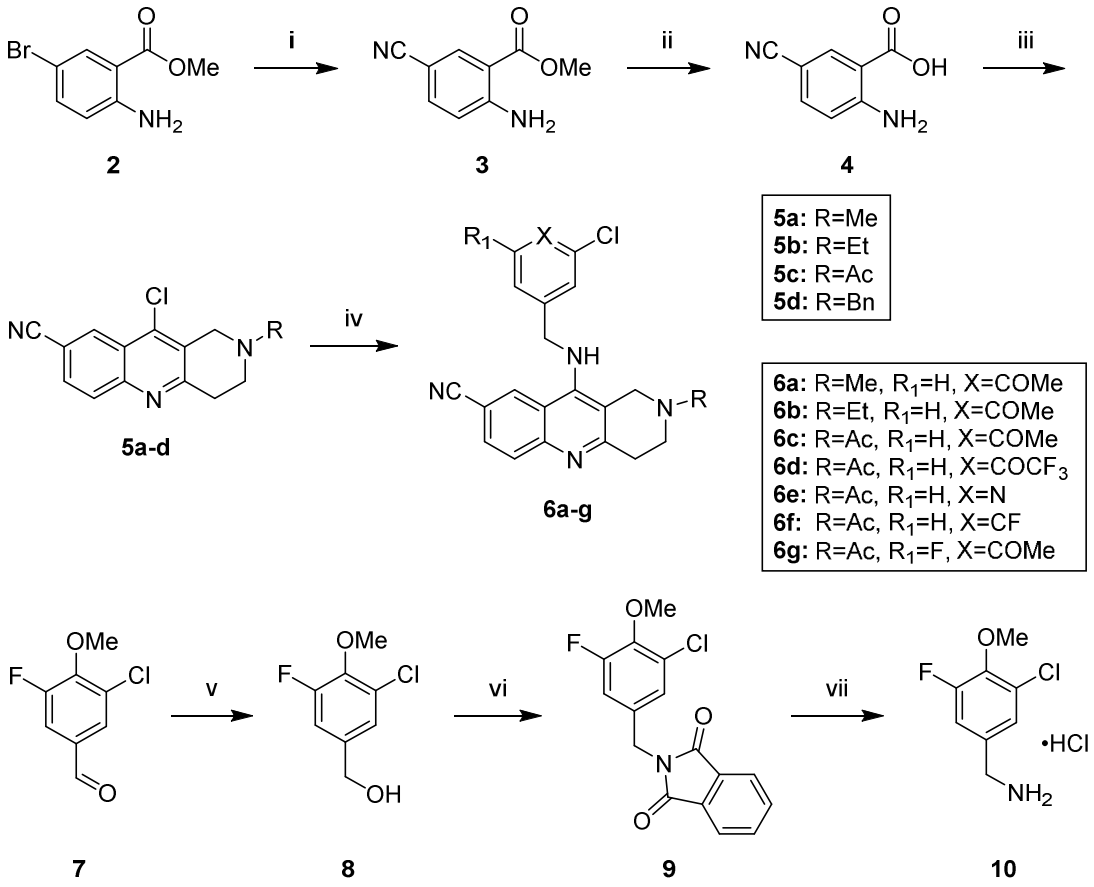

[a]Reagents and conditions: (i) CuCN, NMP, 200 °C, 4h; (ii) EtOH/KOH 1M, 50 °C, 2h; (iii) 1-substituted piperidin-4-one, $POCl_3$, 60 °C, 6h; (iv) Appropriate benzylamine, TEA, NaI, NMP, 130 °C, overnight; (v) $NaBH_4$, THF, r.t., overnight; (vi) phthalimide, DIAD, PPh_3, THF, r.t., 24h; (vii) a) N_2H_4, MeOH, reflux, overnight; b) HCl/Et_2O

Scheme 2. Synthesis of compound 14[a]

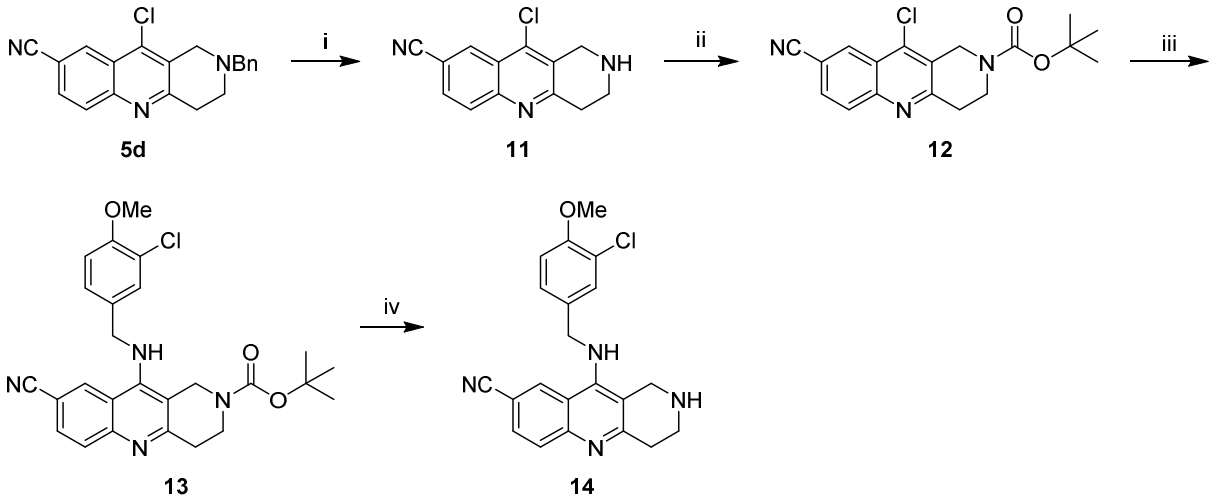

[a]Reagents and conditions: (i) a) ACE-Cl, $ClCH_2CH_2Cl$, reflux; b) MeOH, reflux, 2h; (ii) Boc_2O, CH_2Cl; (iii) 3-chloro-4-methoxybenzylamine, TEA, NaI, NMP, 130 °C, overnight; (iv) Et_2O/HCl 2.0M, CH_2Cl_2,1,4-dioxane, r.t., overnight.

We also sought to introduce other functionalities at the naphthyridine 8-position. In the course of this effort, analogs **17a-d** were synthesized using the same synthetic route of **6a-g** but staring form commercially available materials **15a-c**, as shown in scheme 3.

Scheme 3. Synthesis of compounds 17a-d[a]

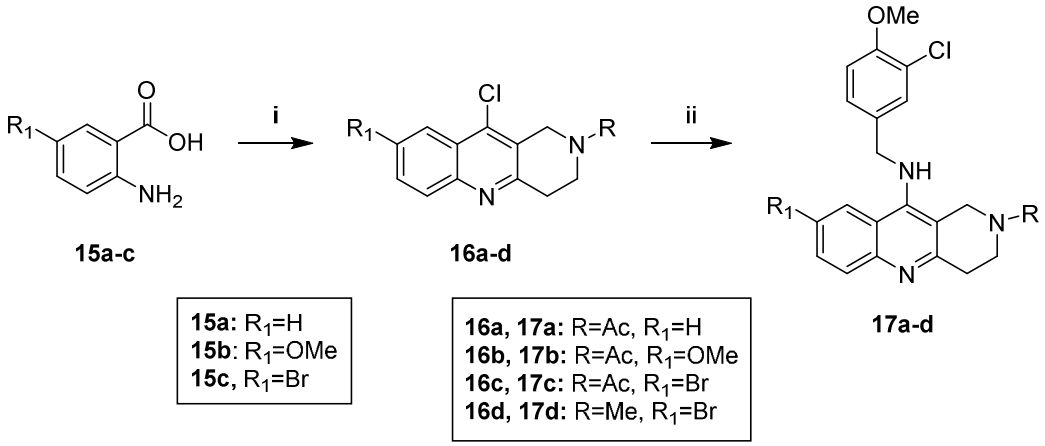

[a]Reagents and conditions: (i) 1-substituted piperidin-4-one, $POCl_3$, 60 °C, 6h; (ii) benzylamine, TEA, NaI, NMP, 130 °C, overnight.

Of note, during the chemical characterization of the naphthyridine-based compounds by ^1H NMR and ^{13}C NMR spectroscopy, the appearance of extra peaks was observed for derivatives bearing the acetyl group at the naphthyridine 2-position. This phenomenon was attributed to the

presence of equilibrating rotamers, which were confirmed by using additional spectroscopic techniques.[24] 1D NOESY experiments allowed us to identify the protons undergoing chemical exchange and to give a clear interpretation of the NMR spectra. A detailed description of the spectroscopic profile of compounds **5c** (Fig. S1 and S2) and **6c** (Fig. S3 and S4) as representative spectra is reported in Supporting Information. In addition, as already reported for our previous series of quinoline-based compounds,[18] a spin-spin coupling between NH protons and their vicinal aliphatic CH_2 protons was observed for most of the naphthyridine-based compounds and confirmed by D_2O exchange. The presence of clear split signals (doublets and triplets) was also depending on the solvent used to record the NMR experiment.

The general synthesis of 1*H*-pyrroloquinolinone analogs **24a-f** is outlined in scheme 4. Starting with 5-substituted 2-aminobenzoic acids **18a-c**, 2*H*-benzo[*d*][1,3]oxazine-2,4(1*H*)-diones **19a-c** were prepared from the reaction with triphosgene. Readily accessible isatoic anhydride **19d** and 5-chloroisatoic anhydride **19e** were utilized for the synthesis of intermediates **20d** and **20e**. Treatment of **19a-e** with methyl acetoacetate yielded the desired methyl 4-oxo-1,4-dihydroquinoline-3-carboxylate derivatives **20a-e**, which were subjected to a chlorination reaction to obtain the 2-methylquinoline derivatives **21a-e**. Next, bromination of the methyl group followed by cyclization with ethylamine in EtOH provided 2,3-dihydro-1*H*-pyrrolo[3,4-*b*]quinolin-1-one derivatives **22a-f**. Introduction of 3-chloro-4-methoxibenzylamine on the tricyclic template via nucleophilic substitution gave the final compound **24a-f**.

Scheme 4. Synthesis of compounds 24a-f[a]

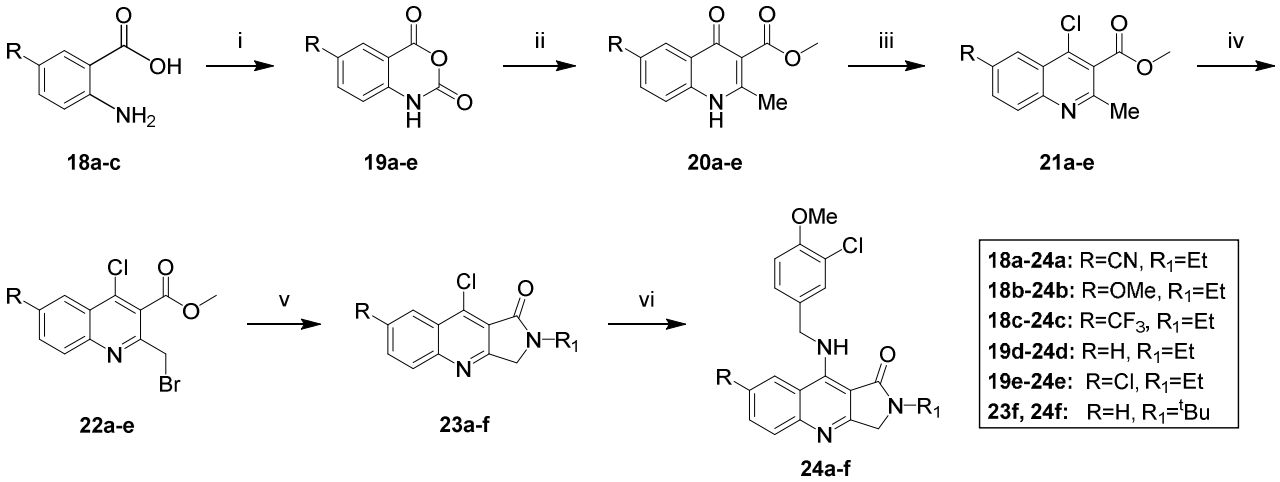

[a]Reagents and conditions: (i) triphosgene, 1,4-dioxane, 90°C, 2h; (ii) methyl acetoacetate, NaH, DMA, 120°C, 20min; (iii) $POCl_3$, 110°C, 30min; (iv) NBS, AIBN, CCl_4, reflux, 4h; (v) ethylamine or *t*ert-butylamine, EtOH, reflux, 2h; (vi) 3-chloro-4-methoxybenzylamine HCl, DIPEA, n-propanol, 90°C, 2h.

Inhibition of PDE5 and selectivity versus PDE6. Both naphthyridine (**6a-g**, **14**, and **17a-d**) and 1*H*-pyrroloquinolinone (**24a-f**) analogs were tested on human recombinant PDE5A1 in a fluorescent enzymatic assay performed by BPS Bioscience (Table 1). With respect to **1**, both scaffold A and B retained potent PDE5 activities. While compounds **6b**, **6g**, and **24c** showed potency comparable to that one of compound **1**, compounds **6c** and **24a** exhibited the highest inhibitory activity in the picomolar range. On the contrary, compounds **6d, 17a** and **24f** displayed the lowest potency, which was still in the nanomolar range. The most potent PDE5Is **6c** and **24a** were also evaluated for selectivity versus PDE6C isozyme, which shares a high similarity in the catalytic site with PDE5 with respect to the molecular binding and therefore represents a major obstacle in developing highly selective PDE5Is.[25] Although both scaffolds were well tolerated, it appears that a larger aliphatic ring fused to the quinoline moiety contributes to increasing the PDE5 selectivity versus PDE6, as compound **6c** bearing a 6-membered aliphatic ring showed to be ~500-fold more potent against PDE5, while the 5-membered fused ring in compound **24a** leads to a selectivity for PDE5 of ~100-fold compared to PDE6.

Table 1. PDE5 and PDE6 activity of naphthyridine and 1*H*-pyrroloquinolinone analogs.

Cmpd	PDE5A1 IC_{50} (nM)[a]	PDE6C IC_{50} (nM)[a]	Cmpd	PDE5A1 IC_{50} (nM)[a]	PDE6C IC_{50} (nM)[a]
1	0.27[b]	339[b]	**17b**	45.2 ± 2.3	n.d.
6a	0.59 ± 0.3	n.d.	**17c**	3.1 ± 0.1	n.d.
6b	0.19 ± 0.01	n.d.	**17d**	21.6 ± 1.0	n.d.
6c	0.056 ± 0.01	30.1 ± 1.1	**24a**	0.059 ± 0.005	6.6 ± 0.3
6d	337 ± 30.5	n.d.	**24b**	3.8 ± 0.3	n.d.
6e	57 ± 6.8	n.d.	**24c**	0.29 ± 0.018	n.d.
6f	1.5 ± 0.2	n.d.	**24d**	64 ± 5.4	n.d.
6g	0.32 ± 0.016	n.d.	**24e**	1.7 ± 0.1	n.d.
14	1.55 ± 0.14	n.d.	**24f**	333 ± 26.3	n.d.
17a	110 ± 3.3	n.d.			

[a]Enzymatic activity was performed by BPS Bioscience using recombinant human enzymes; [b]As reported in reference 18. Values are reported as average ± S.E. (standard error).

Computational study. In order to better understand the structural basis of PDE5 inhibition by the new inhibitors reported here, we have conducted a computational study to identify a binding mode allowing to account for the experimental structure-activity relationship observed within the naphthyridine and the 1*H*-pyrroloquinolinone series (Fig. 1, scaffold A and B respectively).

First, we performed unconstrained *in silico* docking of compounds **6c** and **24a**, the most potent compounds of the naphthyridine and the 1*H*-pyrroloquinolinone series respectively, into the putative cGMP pocket of PDE5A1 (see methods in Experimental Section). We targeted this pocket based on the fact that multiple complex crystal structures show that diverse PDE5 small molecule inhibitors consistently bind in it (e.g., pdb codes 1UHO, 3BJC, 3B2R, 3HDZ, 3SIE, 4G2W, 4G2Y, 4I9Z, 4OEW and 4OEX), showing that it has highly druggable characteristics (Supporting Information, Fig. S5A). The docking pose with the best docking score obtained for

compound **6c** (Fig. 2A and 2B) and compound **24a** (Supporting Information, Fig. S7A) were very consistent (see Supporting Information, Fig. S6A). Interestingly, a second binding mode where the tricyclic ring is flipped compared to the best docking pose described above, was also consistently found for both compounds (Fig. 2C and Supporting Information, Fig. S7B). Of note, the two alternative binding poses occupy approximately the same space within the cGMP pocket for compounds **6c** and **24a,** as the tricyclic ring is rotated by ~180° around its central axis (Supporting Information, Fig. S6C and S6D). Similarly to most PDE5 inhibitors, both compounds lack interaction with the structural Mg^{2+} and Zn^{2+} ions present in the enzymatic pocket.

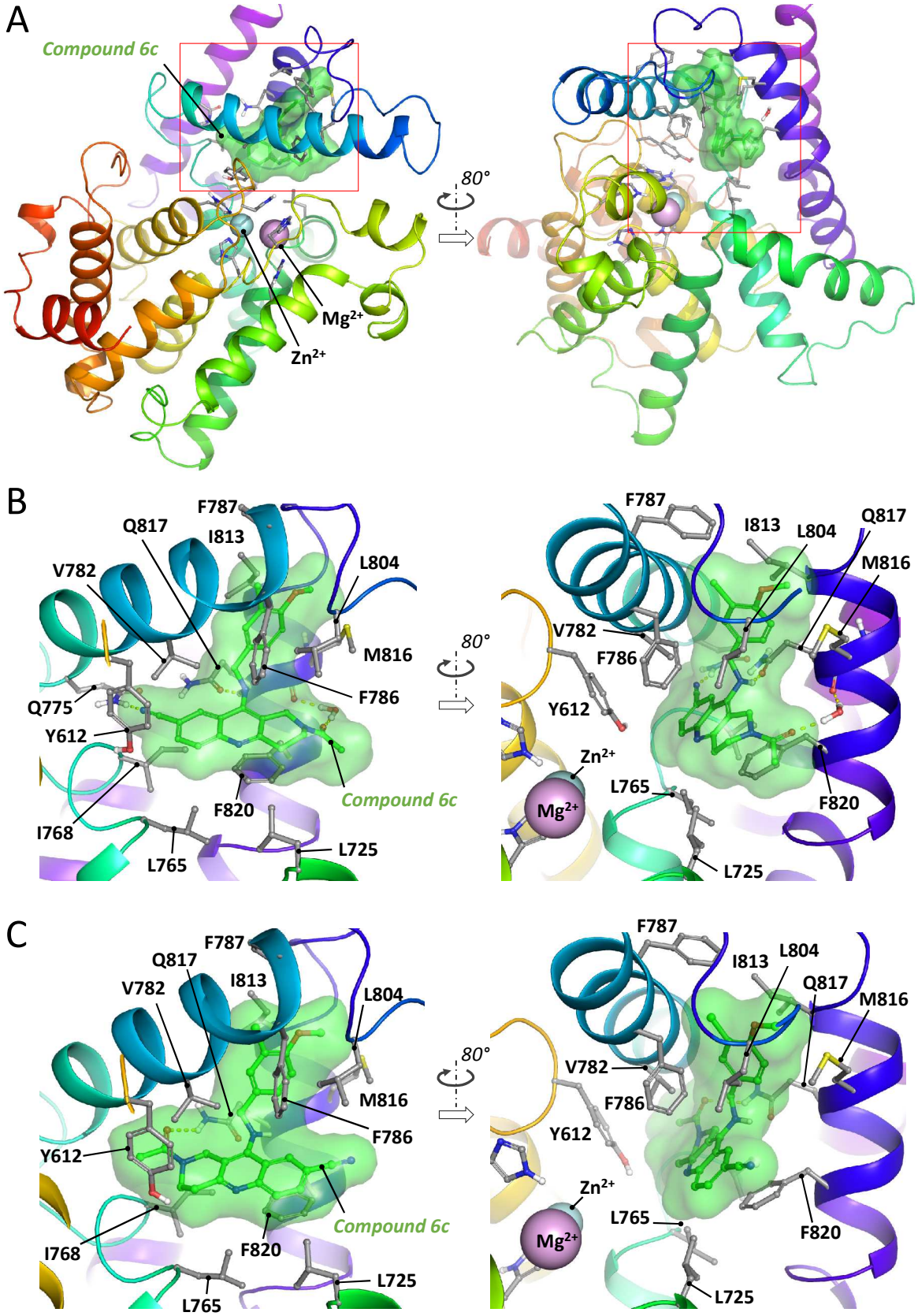
A
Compound 6c
Mg2+
Zn2+
80°
B
F787
Q817
I813
L804
V782
M816
F786
Q775
Y612
I768
F820
L765
L725
Compound 6c
C

Figure 2. Docked binding modes of compound 6c into PDE5 cGMP pocket. (**A**) Overview of PDE5 with compound **6c** docked in the cGMP pocket in its best docking pose. (**B**) Close-up view of the best docking pose for compound **6c**. This pose is very similar to the best docking pose found for compound **24a** (Supporting Information, Fig S6A). Note that for both compounds, post-docking minimization led to a significant change in Q775 side chain orientation compared to the PDB structure used for docking (3TGG). The refined side chain orientation, which optimizes the geometry of the hydrogen bond with the nitrile group of the two compounds, is consistent with an alternative side chain orientations observed for residue Q775 in other PDE5 crystal structures (Supporting Information, Fig. S5B and C). (**C**) Close-up view of the alternative docking pose found for compound **6c**. A very similar alternative docking pose was found for compound **24a** (Supporting Information, Fig S7B). Dashed lines in B and C represent intermolecular hydrogen bonds.

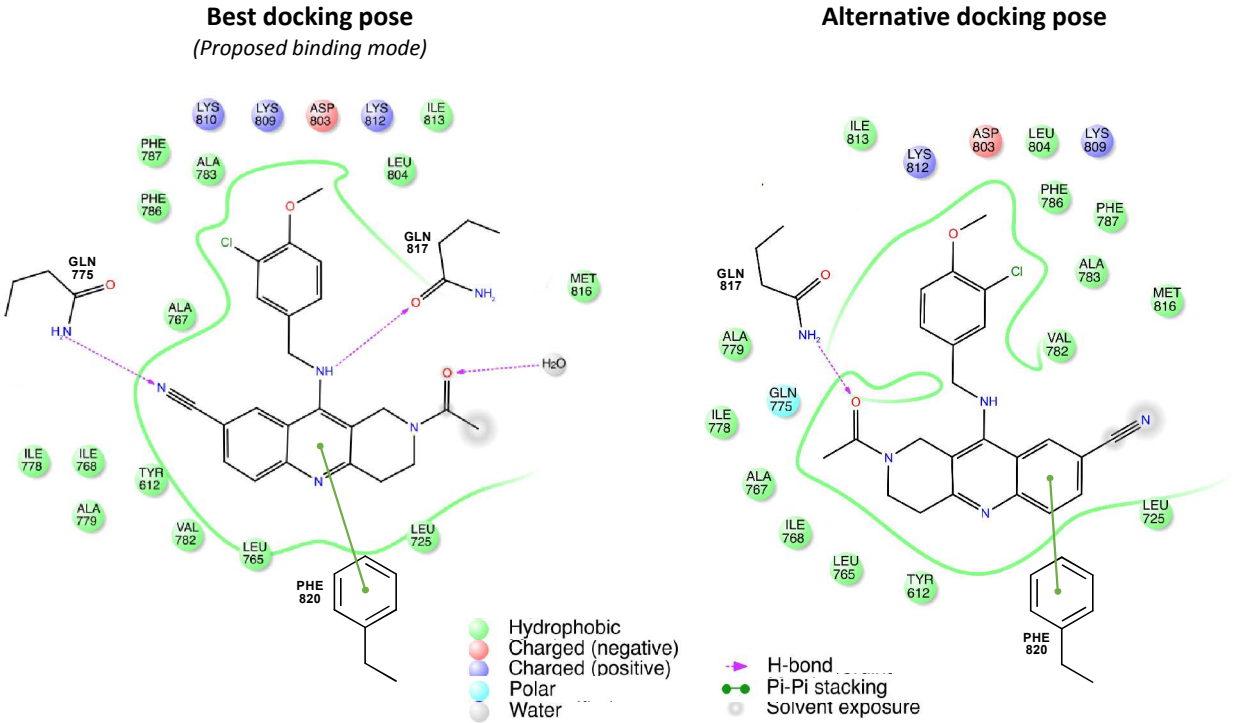

Figure 3. Two-dimensional interaction diagrams for compound 6c. The best docking pose (left) as well as the alternative docking pose (right) are represented. The legend for the residue types and the types of interactions is indicated at the bottom of the figure. The two-dimensional interaction diagrams for compound **24a** are represented in Supporting Information, Fig. S7.

In order to compare these two binding modes and potentially provide further validation for one of them, we explored whether they could account for the structure-activity relationship observed within the naphthyridine and the 1*H*-pyrroloquinolinone series. The interactions of compound **6c** with PDE5 for both binding modes are summarized in Figure 3. Expectedly, the interactions of compound **24a** with PDE5 are very similar for both binding modes (Supporting Information, Fig. S7). Noticeably, these interactions can provide a qualitative explanation for some of the structure-activity relationships observed for the two series of compounds. For the best docking pose, in particular, the hydrogen bond between the nitrile group of compounds **6c** or **24a** and the amide group of residue Q775, located at the deep end of the binding pocket, can explain the significant impact of chemical changes at this position on potency (compare compounds **6c** and **17a-c** for the naphthyridine series and compounds **24a-d** and **24e** for the 1*H*-pyrroloquinolinone series). Among the groups that can be compared for this position, the best potency is obtained with a nitrile group (IC_{50} ~ 0.6 nM for both compound **6c** and **24a**) while the weakest potency, within both series, is obtained in the absence of any acceptor (IC_{50} of 110 nM and 64 nM for compounds **17a** and **24d**, respectively). The presence of a weaker acceptor (e.g., F, Cl or Br in compounds **24c**, **24e** and **17c** respectively) and/or of a shorter linker between the acceptor and the tricyclic ring core (e.g., -OMe in compounds **17b** and **24b** respectively), which places the acceptor further away from the Q775 donor, result in intermediate potencies (Table 1).

On the other side of the tricyclic ring, for the naphthyridine series, the water bridge formed between the acetyl group and M816 backbone in the best docking pose can also explain the reduced potency with groups lacking good acceptor or donor (e.g., IC_{50} of 0.19 nM, 0.59 nM and 1.55 nM with an ethyl group (compound **6b**), methyl group (compound **6a**) and hydrogen (compound **14**) respectively) (Table 1). This role of the acetyl group in the naphthyridine series could however also be explained in the alternative docking pose, by the hydrogen bond formed with residue Q817. In the alternative binding mode, however, the importance of the nitrile group is more difficult to explain as it is mostly solvent exposed.

The two binding modes can also provide an explanation for the importance of the methoxy group in para- position of the benzyl ring of compound **6c** (IC_{50} ~ 0.056 nM for a methoxy group in compound **6c** compared to IC_{50} of 337, 57 and 1.5 nM for a trifluoromethyl, unsubstituted pyridine and a single fluoride in compounds **6d**, **6e** and **6f**, respectively). The benzyl ring carrying the group occupies the same small pocket lined by F786, F787, L804, I813 and M816 in both binding modes (Fig. 2). Performing molecular dynamics simulations, water clustering and statistical thermodynamic analysis using WaterMap[26, 27] shows that in the absence of ligand, this small pocket is likely to be occupied by several "high-energy" water molecules *(i.e.*, predicted by WaterMap to be significantly more energetically stable in the bulk solvent than in the binding pocket, where it however binds in order to avoid vacuum) (Supporting Information. Fig. S8). Overlapping of a ligand with one of these high-energy hydration sites by either a polar or non-polar group allows at the same time to displaces the unstable water into the bulk solvent while avoiding vacuum, and is energetically quite favorable. One of these high-energy hydration sites precisely overlaps with the position of the methoxy group for both docked binding modes of compound **6c** (Supporting Information, Fig. S8), while smaller groups like an unsubstituted

pyridine or a fluoride (compounds **6e** and **6f**) would not be bulky enough to displace this water molecule to the solvent. For the case of the trifluoromethyl substituent (IC_{50} of 337 nM for compound **6d**), the significantly reduced potency can be explained by the fact that while it is certainly bulky enough to desolvate the pocket as well as the methoxy group, its significantly larger size does not sterically fit as well in the pocket.

Overall, these qualitative explanations globally argue rather in favor of the best docking pose relative to the alternative pose, although more work would be needed to further validate one of these poses.

Physicochemical Properties. To determine the potential drug-likeness of compounds **6c** and **24a**, their *in silico* physicochemical properties were evaluated and compared to those of compound **1**. As shown in Table 2, both compounds **6c** and **24a** obey the Lipinski's rule of five and fulfill the restrictions of topological polar surface area (tPSA) for drugs targeting the central nervous system.[28] Additionally, water solubility of compound **6c** and **24a** was assessed to establish whether the new scaffolds showed increased solubility than compound **1**. Kinetic solubility was measured in phosphate buffered saline following an 18-hour incubation period according to the procedure described in the Experimental Section. Compound **24a** was found to have a low kinetic solubility, while compound **6c** showed improved water solubility with respect to compounds **1** (Table 2). Melting point of compound **6c**, **24a**, and **1** has been reported in table 2 as well. These findings suggest that compound **6c** represent a good candidate for further analyses. We then engaged compound **6c** in a set of experiments aimed at evaluating its pharmacological properties and potential use in AD.

Table 2. Water solubility and physicochemical properties of **1**, **6c**, and **24a**.

Cmpds	MW	HBA	HBD	cLogP	tPSA	Water solubility (μM)[a]	Melting point (°C)[b]
1	393.87	5	2	3.42	78.17	<3.9	171.0-173.0
6c	420.90	6	1	3.41	78.25	>500	165.5-167.0
24a	406.87	6	1	3.66	78.25	3.1	207.0-209.0
RO5	<450	<10	<5	<5	<90		

MW: molecular weight, HBA: hydrogen-bond acceptor atoms, HBD: hydrogen-bond donor atoms, clogP: calculated logarithm of the octanol-water partition coefficient, tPSA: topological polar surface area are calculated using http://www.molinspiration.com/cgi-bin/properties; RO5: Lipinski's rule of five; [a]Calculated as turbidimetric (kinetic) solubility by Cyprotex US, LLC; [b]As an average of 2 independent measurements determined on Mel-Temp II, Laboratory devices, USA.

Effects of Compound 6c on Hippocampal cGMP Levels and Synaptic Plasticity. Based on its potency and selectivity profile, as well as its favorable aqueous solubility, compound **6c** was moved into a functional assay aimed at evaluating its ability to increase cGMP levels in the hippocampus of mice. Wild-type (WT) mice were treated with compound **6c** at two different concentrations (3 and 10 mg/kg). Mice were subjected to foot shock and sacrificed 10, 60, and 180 sec afterward (Figure 4). These time points were chosen based on previous experiments in which we observed a change in cGMP levels immediately after foot shock.[18] Increased levels of cGMP were observed at both concentrations and all of the 3 different time points. A dose-dependent increase of cGMP levels was detected in hippocampi collected at 10 and 60 sec after foot shock, with a 1.5- and 1.7-fold increase at 3 and 10 mg/kg, respectively, compared to untreated mice for both time points. At 180 sec, a slight increase in cGMP levels was detected in mice treated with 3mg/kg of **6c** but it failed to reach statistical significance (p=0.097), while the higher dose produced a 1.3-fold increase of cGMP levels with respect to vehicle-treated mice. A compensatory cellular mechanism leading to the hydrolysis of cGMP by other PDEs could

explain the reduced increase of cGMP levels at 180 sec with respect to 60 sec after foot shock for mice treated with 10 mg/kg of compound **6c**. However, longer time points or the employment of inhibitors of other cGMP-hydrolyzing PDEs were not explored to verify this hypothesis. In any case, the NO signal transduction cascade, involving cGMP, is sufficient to phosphorylate CREB that leads to memory formation through transcription of memory-related genes. Such a cellular response is triggered by memory-stimulating events, such as foot shock. Indeed, vehicle-treated mice subjected to foot shock (Fig. 4, veh) showed an increase of cGMP levels compared to vehicle-treated mice that did not receive foot shock (Fig. 4, Basal). Notably, compound **6c** was effective in elevating hippocampal cGMP levels, indirectly proving its ability to cross the blood-brain barrier (BBB).

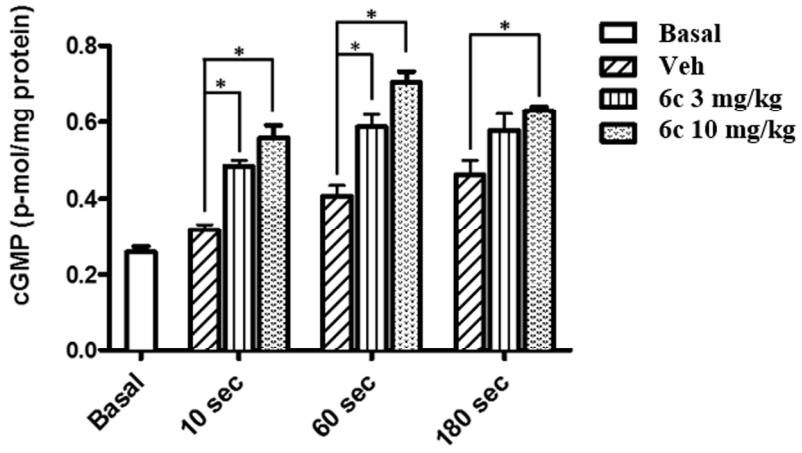

Figure 4. cGMP levels in hippocampus of mice treated with compound 6c at 3 and 10 mg/kg via intraperitoneally. Values are the mean of duplicate determinations. Error bars show S.E.M. (n=3 per group); *p<0.01.

To determine whether compound **6c** was able to strengthen synaptic transmissions, we carried out electrophysiological experiments to measure the compound's effects on hippocampal long-term potentiation (LTP), a type of synaptic plasticity thought to underlie learning and memory

and to be impaired by the elevation of Aβ.[16, 29] Slices of hippocampus were collected from 3-4 month old APP/PS1 transgenic mice and WT littermate controls and were treated either with vehicle or **6c** (50 nM through the bath perfusion for 10 min prior to the tetanus) (Fig. 5A and B). According to our previous results, vehicle-treated APP/PS1 mice showed a reduction in LTP compared to WT mice.[30] Compound **6c** rescued the defect in LTP; residual potentiation recorded in slices from APP/PS1 mice treated with compound **6c** (201.76% ±14.09) was increased with respect to slices from APP/PS1 mice treated with vehicle (137.30% ±10.83) (Fig. 5A and B). Compound **6c** did not have any effect on WT slices, consisting with the possibility that the inhibitor is acting on the LTP mechanisms underlying memory loss instead of a more generalized effect (Fig. 5A and B). Thus, by acting on the NO/cGMP signaling pathway, compound **6c** re-established the normal increase of synaptic strength in the hippocampus of APP/PS1 mice (Fig. 5A and B). A similar beneficial effect was observed when compound **6c** was injected to APP/PS1 mice from the age of 3-4 months for 3 weeks and hippocampal slices were harvested at 6-7 months of age (Fig. 5C and D). LTP was restored in compound-treated APP/PS1 mice (226.22% ±6.71) compared to non-treated transgenic mice (164.11% ±10.36) (Fig. 5C and D), suggesting an enduring effect of **6c** on potentiating synaptic plasticity. These results corroborate our previous findings on the prolonged beneficial effect induced by the PDE5 inhibition on synaptic and cognitive abnormalities in APP/PS1 mice that persists beyond the administration of the inhibitor.[18, 17]

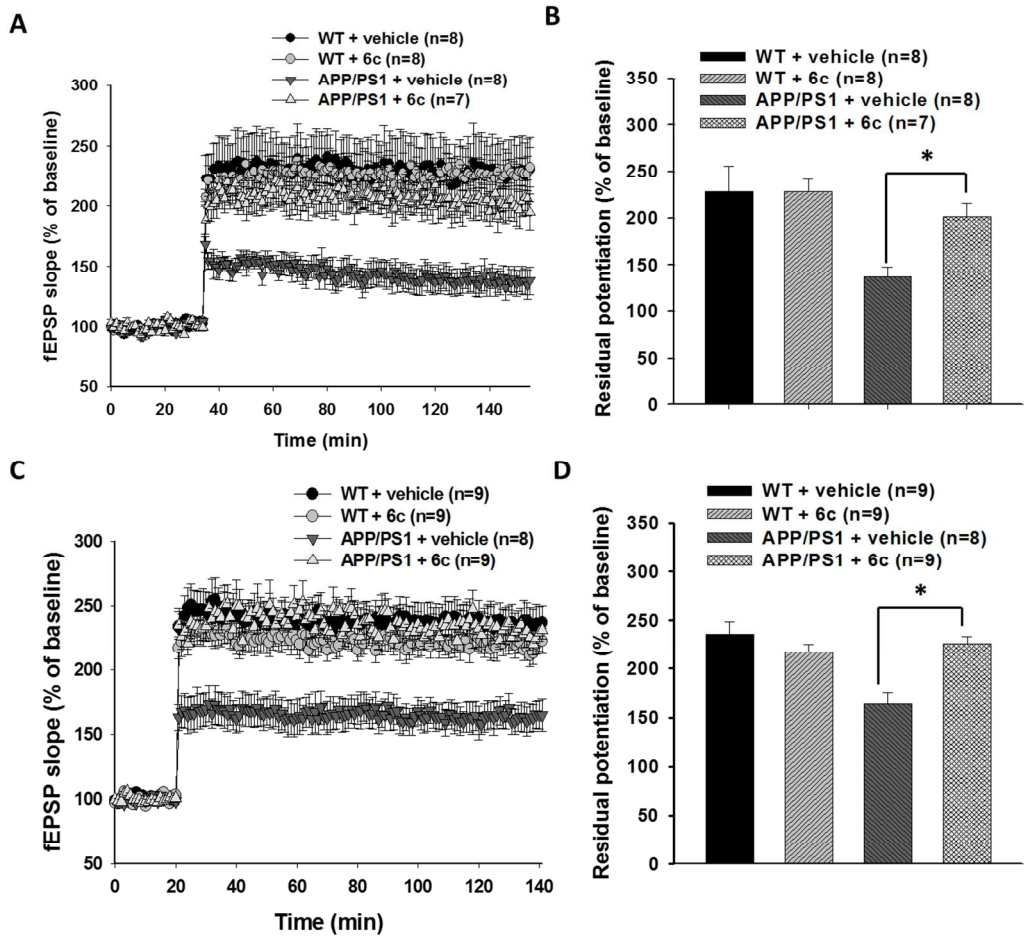

Figure 5. Beneficial effect of compound 6c on synaptic deficits in APP/PS1 mice. Two hours recording following tetanic stimulation of the Schaffer collateral fibers at the CA3-CA1 connection. **A)** Slices were prepared from 3-month-old WT and APP/PS1 mice treated with vehicle or compound **6c** at 50nM (acute perfusion, *$p<0.01$ and $F_{(1,13)}=15.57$). **B)** Residual potentiation recorded during the last 5 minutes of a 2 hr recording shown in panel A; **C)** Daily treatment with compound **6c** (3mg/kg, i.p.) for 3 weeks at the age of 3-4 months, slices were recorded at 6-7 months of age; *$p<0.01$ and $F_{(1,15)}=27.0$; **D)** Residual potentiation recorded during the last 5 minutes of a 2 hr recording shown in panel C.

Plasma and Brain Levels and *in vitro* Microsomal Stability of Compound 6c. To further validate compound **6c** as a promising candidate for treating a central nervous disease, a

pharmacokinetic study was performed. We evaluated brain and plasma levels in mice after intraperitoneal (i.p.) administration of compound **6c** at 25 mg/kg at different time points (0, 5, 15, 30, 60, and 120 min). As shown in Table 3, peak plasma concentration of **6c** occurred 0.25 h after dosing and its plasma half-life was 1.07 h. At 0.25 h, concentration of **6c** in the brain and plasma were 492.25 ng/g and 1571.44 ng/mL, respectively. The logBB value was used to evaluate BBB permeability; **6c** showed the logBB values of −0.50, which was within the established threshold that defines a compound as crossing the BBB (logBB ≥ −1).[31] Therefore, compound **6c** demonstrated to cross the BBB.

Table 3. Plasma and brain concentrations, logBB, half-life, and *in vitro* microsomal stability of compound **6c**.

Sample	Plasma [a] (ng/mL)	Brain [a] (ng/g)	LogBB[b]	Half-life [a] (h)	Microsomal stability[c] (min)
n=3	1571.44	492.25	−0.50	1.07	6.0 (HLM) 3.2 (MLM)

[a]Values determined 0.25 h after administration; [b]BB: ratio of the brain to plasma concentration; [c]Microsomal stability was performed by Absorption Systems.

Microsomal stability of compound **6c** was measured in both mouse liver microsomes (MLM) and human liver microsomes (HLM) (Table 3). Such short half-lives were indicative of a rapid metabolism of the compound by both mouse and human microsomes. Optimizing the metabolic stability while maintaining potency is an effort to be pursued in a following study. The structural insights gained through the computational study presented above will be leveraged in this endeavor. A first possible metabolic liability to be further explored is the de-methylation of the methoxy group on the benzyl ring of compound **6c**. If this metabolic liability is confirmed (for example through microsomal stability profiling of compounds **6d**, **6e** and **6f**), the binding mode

proposed for compound 6c will be used to guide the choice of an isostere to replace the methoxy group (*i.e.* bulky enough to desolvate the pocket while not too bulky to sterically fit well in it).

Behavioral Studies of Compound 6c. Despite analysis of microsomal stability suggested that further improvement is needed, we wanted to verify if the new scaffold (compound **6c**) retained the capability of rescuing the memory loss in the APP/PS1 mouse model of AD. To this end, two memory tasks fear conditioning (FC) and 2-day radial arm water maze (RAWM) were performed to assess associative and spatial memory, respectively (Fig. 6). APP/PS1 mice were subjected to both tasks at the age of 3-4 month (Fig. 6, A and B), when they clearly show cognitive impairment.[30, 32] In these experiments, both APP/PS1 and WT mice were treated with **6c** (3 mg/kg, i.p.) daily for 3 weeks and compared to vehicle-treated APP/PS1 and WT mice. Percentage of freezing in the FC task (Fig. 6A) defines the animal response to an electric foot shock (see Experimental Section for detailed methods). Figure 6A shows that vehicle-treated transgenic mice froze less (~15% freezing) compared to vehicle- and compound-treated WT mice as well as compound-treated APP/PS1 mice, indicating the inability of these animals to associate the noxious stimulus with the environment where the stimulus occurs. Treatment with **6c**, on the other hand, rescued contextual learning in APP/PS1 mice (~30% freezing) without affecting memory in WT mice (~30% freezing). In the 2-day RAMW (Fig. 6B), the number of errors refers to the ability of the animal to reach the hidden platform, which is placed in one of the 6 arms of a maze (see Experimental Section for detailed methods). Compared to vehicle-treated APP/PS1 (~3 errors), compound-treated APP/PS1 showed a fewer number of errors (~1 error) suggesting that compound **6c** is able to rescue spatial working memory. As expected,

vehicle- and compound-treated WT mice performed well in the 2-day RAWM as they show no symptoms of memory impairment.

To investigate whether the beneficial effects of compound **6c** on synaptic and cognitive abnormalities in APP/PS1 mice was persisting beyond its administration, both WT and APP/PS1 mice that were treated for 3 weeks with **6c** at the age of 3 months were assessed for contextual and spatial memory when they were 6-7 month old (Fig. 6, C and D). In the contextual memory experiments, transgenic mice treated with the compound froze ~40% of the time compared to ~15% in vehicle-treated transgenic mice (Fig. 6C) and made ~1 error in the 2-day RAWM test compared to ~2.5 in vehicle-treated transgenic mice (Fig. 6D). Thus, synaptic and cognitive improvements persist beyond the administration of compound **6c**. For all experiments, we performed cued conditioning and visible platform tasks to verify that contextual memory-independent mechanisms interfere with the interpretation of the results. None of these controls showed differences among various groups of mice (see Supporting Information, Figures S9 and S10).

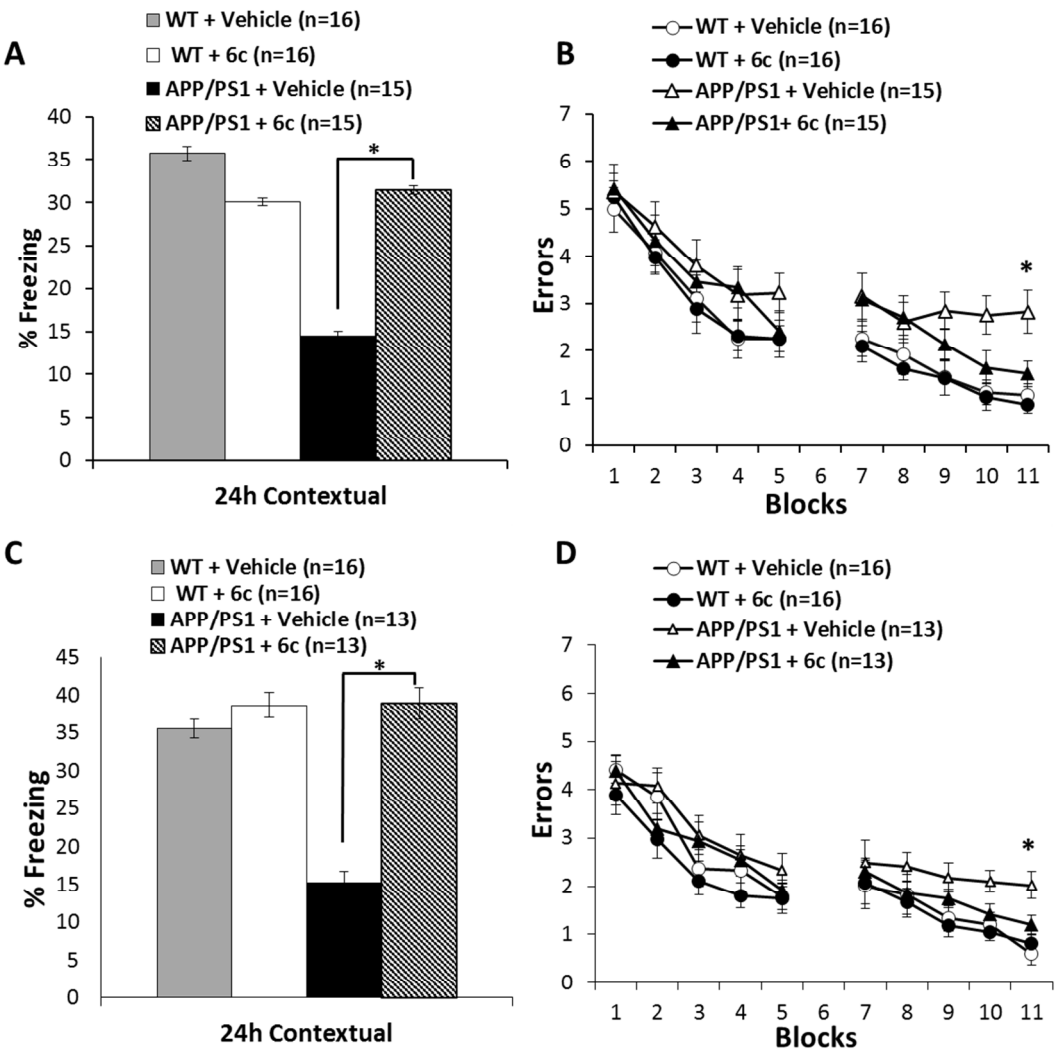

Figure 6. Beneficial effect of compound 6c on cognitive deficits in APP/PS1 mice. A) Daily treatment with compound **6c** (3mg/kg, i.p.) for 3 weeks at the age of 3-4 month re-established normal freezing in a test for contextual fear memory. **B)** Daily treatment with compound 6c (3mg/kg, i.p.) for 3 weeks at the age of 3-4 months reduced the number of errors with the 2-day radial arm water maze. **C)** Daily treatment with compound **6c** (3mg/kg, i.p.) for 3 weeks at the age of 3-4 months re-established normal freezing in a test for contextual fear memory when mice were examined at 6-7 months of age. **D)** Daily treatment with compound **6c** (3mg/kg, i.p.) for 3

weeks at the age of 3-4 months reduced the number of errors with the 2-day radial arm water maze when mice were examined at 6-7 months of age. * $p < 0.05$

CONCLUSION

We reported an extensive study of new chemical entities with PDE5 inhibitory activity. In particular, we reported the naphthyridine derivative **6c**, which was found to have excellent PDE5 potency and selectivity, with improved water solubility with respect to the quinoline analog **1**.[18] Despite its lack of *in vitro* metabolic stability, which suggests the need of further effort toward the optimization of this drug property, physicochemical and pharmacological properties of compound **6c** were found to be optimal for a potential drug candidate.

Using *in silico* docking, we were furthermore able to identify two plausible binding modes and provide structural insights into the structure-activity relationship for the two series of compounds reported here. Further validation of one of these binding modes is work for a following study and should open the way to the structure-based optimization of the compounds reported here.

We further showed that treatment with compound **6c** increased cGMP levels in the hippocampus of mice and improved learning and memory deficits in a mouse model of AD. These findings strengthen the hypothesis that the NO/cGMP/PKG/CREB molecular pathway plays an important role in learning and memory and that the inhibition of PDE5 represents a sound AD therapeutic approach for either slowing down or preventing the progress of the disease.

EXPERIMENTAL SECTION

Chemistry. General Method. All solvents and chemicals were reagent grade. Unless otherwise mentioned, all reagents and solvents were purchased from commercial vendors and used as received. Silica gel chromatography was performed using glass columns packed with silica gel (200−400 mesh, Aldrich Chemical). ^{1}H and ^{13}C NMR spectra were recorded on an Agilent-NMR-vnmrs400 (400 MHz and 100 MHz, respectively) spectrometer and were determined in chloroform-d, DMSO-d6, acetone-d6 or methanol-d4 with tetramethylsilane (TMS) (0.00 ppm) or solvent peaks as the internal reference. Chemical shifts (δ) are reported in ppm relative to the reference signal, and coupling constant (*J*) values are reported in Hertz (Hz), multiplicity (s = singlet, d = doublet, dd = double doublet, t = triplet, q = quartet, m = multiplet, br = broad). The purity of all final compounds was ≥ 95 % and was determined by LC/MS at wavelengths 220 and 254 nm. Liquid chromatography-mass spectrometry (LC/MS) was performed on two different instruments, a Shimadzu 2010A and a Shimadzu 2020 UFLC mass spectrometer, using a Waters Sunfire column (C18, 5μm, 2.1 mm x 50 mm, a linear gradient from 5 % to 100 % B over 15 min, then 100 % B for 2 min (A = 0.1 % formic acid + H_2O, B = 0.1 % formic acid + CH_3CN), flow rate 0.2000 mL/min). HRMS (ESI) was performed by Furong Sun and associates at the University of Illinois (Urbana-Champaign). Thin layer chromatography (TLC) was performed on EMD precoated silica gel 60 F254 plates, and spots were visualized with UV light (254 nm). All reagents and solvents were used as received from major commercial suppliers, such as Sigma-Aldrich, Fisher Scientific, and Alfa Aesar without further purification. All air- or moisture-sensitive reactions were run under an atmosphere of argon in oven-dried glassware unless otherwise noted.

General procedure A for the synthesis of 10-chloro-1,2,3,4-tetrahydrobenzo[*b*][1,6]naphthyridine. *N*-subtituted piperidin-4-one (1 equiv) and 5-

substituted 2-aminobenzoic acid (1 equiv) were heated to 60 ^{0}C in $POCl_3$ (which was used as a reagent and a solvent) for 6h. The excess of $POCl_3$ was evaporated off and the residue was treated with iced H_2O and NaOH 10% (till pH alkaline) and extracted with CH_2Cl_2. The organic layers were combined and dried over Na_2SO_4, filtered and evaporated under reduced pressure. Residue was purified by column chromatography on silica gel.

General procedure B for nucleophilic substitution on 10-chloro-1,2,3,4-tetrahydrobenzo[*b*][1,6]naphthyridine. A mixture of 10-chloro-1,2,3,4-tetrahydrobenzo[*b*][1,6]naphthyridine (1 equiv), benzylamine (3 equiv), TEA (3 equiv) and NaI (0.1 equiv) in NMP was heated to 130 °C overnight. The mixture was diluted with CH_2Cl_2 and washed with H_2O twice and brine once. The organic layers were dried over Na_2SO_4, filtered and evaporated under reduced pressure. The residues were purified by column chromatography on silica gel.

General procedure C for the synthesis of 2*H*-benzo[*d*][1,3]oxazine-2,4(1*H*)-dione. Triphosgene (1 equiv) was added to a suspension of 5-substituted 2-amino-benzoic acid (3 equiv) in 1,4-dioxane at 0 °C. The homogeneous reaction mixture was heated to 90 °C for 2h and then cooled down. The resulting precipitate was isolated by filtration.

General procedure D for formation of 4-oxo-1,4-dihydroquinoline-3-carboxylate. NaH (1.2 equiv) was added portion wise to a solution of methyl acetoacetate (1.2 equiv) in DMA. 2*H*-benzo[*d*][1,3]oxazine-2,4(1*H*)-dione (1 equiv) was added and the reaction mixture was stirred to 120 ^{0}C for 30 min. The solvent was reduced and water was added. The resulting precipitate was collected by filtration.

General procedure E for chlorination of methyl 4-oxo-1,4-dihydroquinoline-3-carboxylate. Methyl 4-oxo-1,4-dihydroquinoline-3-carboxylate was suspended in $POCl_3$ and heated to 110 °C for 30 min. The homogeneous reaction mixture was slowly poured into iced NH_3 aq. and the aqueous phase was extracted with AcOEt (3x 50 mL). The organic layers were dried over Na_2SO_4, filtered and evaporated under reduce pressure to give the desire compound.

General procedure F for bromination of methyl 2-methylquinoline-3-carboxylate. A solution of methyl 2-methylquinoline-3-carboxylate (1.0 equiv), N-bromosuccinimide (1.5 equiv) and 2,2'-Azobis(2-methylpropionitrile) (0.2 equiv) in CCl_4 was heated to reflux for 4h. The reaction mixture was cooled down and the solid was filtered off. The filtrate was concentrated and the residue was purified by flash chromatography.

General procedure G for formation of 2,3-dihydro-1*H*-pyrrolo[3,4-*b*]quinolin-1-one. $EtNH_2$ (2M in THF, 3.0 equiv) or *tert*-butylamine (2M in THF, 3.0 equiv) was added to a solution of methyl 2-(bromomethyl)-4-chloroquinoline-3-carboxylate (1.0 equiv) in ethanol. The reaction mixture was heated to reflux for 2h. The solvent was evaporated off and the residue was purified by flash chromatography to give the desired compound.

General procedure H for nucleophilic substitution on 2,3-dihydro-1*H*-pyrrolo[3,4-*b*]quinolin-1-one. A solution of 2,3-dihydro-1*H*-pyrrolo[3,4-*b*]quinolin-1-one (1.0 equiv), 3-chloro-4-methoxybenzylamine hydrochloride (1.5 equiv) and DIPEA (6.0 equiv) in *n*-propanol was heated to 90 °C for 2h. After cooling down, the resulting precipitate was collected by filtration.

Methyl 2-amino-5-cyanobenzoate (3). A mixture of **2** (21.72 mmol) and CuCN (26.07 mmol) in NMP was stirred for 5h at 210 °C. After cooling the reaction down, the mixture was

poured into a 15 mL of an aqueous solution of $FeCl_3$ (15.0 g) and conc. HCl (2.2 mL). The resulting mixture was stirred at 60 °C for 1h and then cooled to room temperature. AcOEt was added and the mixture washed with 1N NaOH solution (3 times) and brine (1 time). The organic layer was dried over Na_2SO_4, filtered and evaporated under reduced pressure to give a dark solid, which was purified by flash chromatography using ethyl acetate. White solid; yield 56%; ^{1}H NMR (400 MHz, $CDCl_3$) δ 8.19 (d, 1H, *J*=2.0 Hz), 7.45 (dd, 1H, *J*= 8.4, 2.0 Hz), 6.6 (d, *J*= 8.8 Hz), 6.28 (br s, 2H, NH_2), 3.89 (s, 3H).

2-Amino-5-cyanobenzoic acid (4). **3** (17.0 mmol) was dissolved in EtOH (3 mL) and KOH 1M (10 mL) was added. The reaction was heated to 50 °C for 2h. After cooling the reaction down, HCl conc. was added to a pH= 6-7 and the resulting precipitate **4** (off-white solid) was collected by filtration. Compound **4** was used without further purification. Crude yield 96%.

10-Chloro-2-methyl-1,2,3,4-tetrahydrobenzo[*b*][1,6]naphthyridine-8-carbonitrile (5a). Following general procedure A, 1-methylpiperidin-4-one and **4** provided **5a**; column chromatography using ethyl acetate/methanol, 95/5; yield 55%; ESI-MS m/z 286 $[M+H]^+$; ^{1}H NMR (400 MHz, $CDCl_3$) δ 8.58 (s, 1H), 8.07 (d, 1H, *J*= 8.7 Hz), 7.83 (d, 1H, *J*= 8.7 Hz), 3.85 (s, 2H), 3.30 (t, 2H, *J*= 6.0 Hz), 2.89 (t, 2H, *J*= 6.0 Hz), 2.60 (s, 3H).

10-Chloro-2-ethyl-1,2,3,4-tetrahydrobenzo[*b*][1,6]naphthyridine-8-carbonitrile (5b). Following general procedure A, 1-ethylpiperidin-4-one and **4** provided **5b**; column chromatography using methylene chloride/methanol, 95/5; yield 26%; ESI-MS m/z 286 $[M+H]^+$; ^{1}H NMR (300 MHz, $CDCl_3$) δ 8.58 (d, 1H, *J*= 1.8 Hz), 8.06 (d, 1H, *J*= 8.7 Hz), 7.82 (dd, 1H, *J*= 8.4, 1.8 Hz), 3.91 (s, 2H), 3.30 (t, 2H, *J*= 5.7 Hz), 2.93 (t, 2H, *J*= 5.7 Hz), 2.75 (q, 2H, *J*= 7.2 Hz), 1.26 (t, 3H, *J*= 7.2 Hz).

2-Acetyl-10-chloro-1,2,3,4-tetrahydrobenzo[*b*][1,6]naphthyridine-8-carbonitrile (5c). Following general procedure A, 1-acetylpiperidin-4-one and **4** provided **5c**; column chromatography using methylene chloride/methanol, 95/5; yield 38%. ESI-MS m/z 286 $[M+H]^+$; ^{1}H NMR (400 MHz, $CDCl_3$): (mixture of rotamers) δ 8.61 (s, 1H), 8.13-8.08 (m, 1H), 7.88-7.85 (m, 1H), 5.02 and 4.89 (2 s, 2H), 4.03 and 3.90 (2 t, 2H, *J*=6.0 Hz), 3.30 and 3.24 (2 t, 2H, *J*=6.0 Hz), 2.28 and 2.27 (2 s, 3H); ^{13}C NMR (100 MHz, $CDCl_3$): (mixture of rotamers) δ 169.57, 169.34, 160.14, 159.03, 148.03, 147.76, 140.42, 139.71, 130.94, 130.75, 130.57, 130.39, 130.15, 130.03, 127.09, 126.18, 124.93, 124.62, 118.24, 111.02, 110.96, 46.36, 43.23, 42.47, 38.73, 33.89, 33.03, 21.81, 21.44.

2-Benzyl-10-chloro-1,2,3,4-tetrahydrobenzo[*b*][1,6]naphthyridine-8-carbonitrile (5d). Following general procedure A, 1-benzylpiperidin-4-one and **4** provided **5d**; column chromatography using hexane/ethyl acetate, 50/50; yield 54%; ESI-MS m/z 334 $[M+H]^+$; ^{1}H NMR (300 MHz, $CDCl_3$) δ 8.56 (d, 1H, *J*=1.8 Hz), 8.04 (d, 1H, *J*= 8.7 Hz), 7.82 (dd, 1H, *J*=8.7, 1.8 Hz), 7.43-7.31 (m, 5H), 3.93 (s, 2H), 3.83 (s, 2H), 3.26 (t, 2H, *J*= 6.0 Hz), 2.92 (t, 2H, *J*=6.0 Hz).

10-[(3-Chloro-4-methoxybenzyl)amino]-2-methyl-1,2,3,4-tetrahydrobenzo[*b*][1,6]naphthyridine-8-carbonitrile (6a). Following general procedure B, 3-chloro-4-methoxibenzylamine HCl and **5a** provided **6a**; Column chromatography using ethyl acetate/methanol, 90/10); yield 33%; ESI-HRMS (m/z) $[M + H^+]$ calcd for $C_{22}H_{22}N_4OCl$: 393.1482, Observed: 393.1487; LCMS Purity 99.2%, Rt = 6.6 min; ^{1}H NMR (400 MHz, $CDCl_3$) δ 8.32 (d, 1H, *J*= 1.6 Hz), 7.96 (d, 1H, *J*= 8.8 Hz), 7.71 (dd, 1H, *J*= 8.4, 1.6 Hz), 7.37 (d, 1H, *J*= 2.4 Hz), 7.18 (dd, 1H, *J*= 8.8, 2.4 Hz), 6.94 (d, 1H, *J*= 8.4 Hz), 4.57 (d, 2H, *J*= 6.4 Hz, NH$\underline{CH_2}$), 4.08 (t, 1H, *J*= 6.0 Hz, $\underline{NH}CH_2$), 3.92 (s, 3H, OCH_3), 3.53 (s, 2H), 3.21 (t, 2H, *J*= 5.8 Hz), 2.83

(t, 2H, *J*= 5.8 Hz), 2.52 (s, 3H, $COCH_3$); ^{13}C NMR (100 MHz, $CDCl_3$) δ 159.26, 154.87, 149.02, 148.67, 131.64, 130.40, 129.59, 129.47, 129.33, 126.98, 122.96, 119.40, 119.28, 115.68, 112.41, 107.17, 56.21, 54.23, 52.60, 52.16, 46.22, 33.86.

10-[(3-Chloro-4-methoxybenzyl)amino]-2-ethyl-1,2,3,4-tetrahydrobenzo[*b*][1,6]naphthyridine-8-carbonitrile (6b). Following general procedure B, 3-chloro-4-methoxibenzylamine HCl and **5b** provided **6b**; Column chromatography using ethtla acetate/methanol, 95/5; yield 38%; ESI-HRMS (m/z) [M + H^+] calcd for C_{23} H_{24} N_4 O Cl: 407.1639, Observed: 407.1658; LCMS Purity 99.5%, Rt = 6.67 min; ^1H NMR (400 MHz, $CDCl_3$) δ 8.31 (d, 1H, *J*= 1.2 Hz), 7.96 (d, 1H, *J*= 8.8 Hz), 7.71 (dd, 1H, *J*=8.8, 1.6 Hz), 7.37 (d, 1H, *J*= 2.0 Hz), 7.17 (dd, 1H, *J*=8.0, 2.0 Hz), 6.93 (d, 1H, *J*= 8.8 Hz), 4.56 (d, 2H, *J*= 6.4 Hz, $NH\underline{CH_2}$), 4.12 (t, 1H, *J*= 5.2 Hz, $\underline{NH}CH_2$), 3.92 (s, 3H, OCH_3), 3.57 (s, 2H), 3.21 (t, 2H, *J*= 6.0 Hz), 2.86 (t, 2H, *J*= 6.0 Hz), 2.64 (q, 2H, *J*= 7.4 Hz, $\underline{CH_2}CH_3$), 1.18 (t, 3H, *J*= 7.0 Hz, $CH_2\underline{CH_3}$). ^{13}C NMR (100 MHz, $CDCl_3$) δ 159.80, 154.86, 149.00, 148.84, 131.75, 130.40, 129.51, 129.42, 129.32, 126.93, 123.00, 119.51, 119.29, 116.04, 112.42, 107.21, 56.22, 52.64, 52.10, 51.97, 49.61, 33.81, 12.35.

2-Acetyl-10-[(3-chloro-4-methoxybenzyl)amino]-1,2,3,4-tetrahydrobenzo[*b*][1,6]naphthyridine-8-carbonitrile (6c). Following general procedure B, 3-chloro-4-methoxibenzylamine HCl and **5c** provided **6c**; Column chromatography using ethyl acetate/methanol, 95/5; yield 20%; ESI-HRMS (m/z) [M + H^+] calcd for C_{23} H_{22} N_4 O_2 Cl: 421.1431, Observed: 421.1429; LC/MS Purity 96.79%, Rt = 8.075; ^1H NMR (400 MHz, $CDCl_3$): (mixture of rotamers) δ 8.32 and 8.33 (1H, 2 s), 8.01 and 7.94 (1H, 2 d, *J*=8.7 Hz), 7.77 and 7.70 (1H, d, *J*=8.8 Hz and dd, *J*=9.0, 1.5 Hz), 7.36 and 7.28 (1H, s and d, *J*=2.1 Hz), 7.18 and 7.13 (1H, dd, *J*=8.4, 2.1 Hz and d, *J*=8.4 Hz) , 6.92 and 6.91 (1H, 2 d, *J*=8.0 Hz), 4.68 and 4.53 (2H,

2 s), 4.62 (d, 2H, *J*=6.0 Hz), 4.43 (br s, 1H, NH), 3.9 and 3.79 (2H, 2 t, *J*=6.4 Hz), 3.88 (s, 3H), 3.17 and 3.13 (2H, 2 t, *J*=6.0 Hz), 2.18 and 2.03 (2H, 2 s); ^{13}C NMR (100 MHz, $CDCl_3$): (mixture of rotamers) δ 169.63, 169.03, 159.80, 158.27, 154.93, 149.07, 148.76, 131.54, 131.26, 130.69, 130.44, 129.92, 129.75, 129.71, 129.38, 129.25, 129.00, 126.92, 126.73, 123.27, 123.03, 119.91, 119.40, 119.04, 114.09, 113.36, 112.53, 56.24, 56.19, 52.69, 52.47, 44.70, 43.38, 40.13, 39.16, 33.85, 33.08, 21.59, 21.47.

2-Acetyl-10-[3-chloro-4-(trifluoromethoxy)benzyl]amino-1,2,3,4-tetrahydrobenzo[*b*][1,6]naphthyridine-8-carbonitrile (6d). Following general procedure B, 3-chloro-4-(trifluoromethoxy)-benzenemethanamine and **5c** provided **6d**; Column chromatography using ethyl acetate/methanol, 95/5; yield 37%; ESI-HRMS (m/z) [M + H^+] calcd for C_{23} H_{19} N_4 O_2 Cl F_3: 475.1149, Observed: 475.1161; LC/MS Purity 97.74%, Rt = 8.91 min; ^{1}H NMR (400 MHz, $CDCl_3$): (mixture of rotamers) δ 8.31 (d, 1H, *J*=1.2 Hz), 8.04 and 7.99 (2 d, 0.75H, *J*=8.8 Hz), 7.75 (dd, 1H, *J*=8.6, 1.6 Hz), 7.48 (d, 1H, *J*=2.0 Hz), 7.35 (dd, 1H, *J*=8.4, 0.8 Hz), 7.30 (dd, 1H, *J*=8.4, 2.4 Hz), 4.74 and 4.58 (2 s, 2H), 4.70 and 4,64 (2 d, 1.5H, $\underline{CH_2}$NH, *J*= 6.8 Hz), 4.52 (s, 1H, NH), 3.94 and 3.83 (2 t, 2H, *J*=6.4 Hz), 3.22 and 3.17 (2 t, 2H, *J*=6.4 Hz), 2.21 and 2.04 (s, 3H); ^{13}C NMR (100 MHz, $CDCl_3$): (mixture of rotamers) δ 169.72, 168.94, 158.58, 149.03, 148.71, 144.94, 138.71, 138.43, 130.88, 130.64, 130.03, 129.82, 129. 80, 129.62, 129.28, 129.49, 128.11, 126.74, 126.48, 123.30, 123.11, 121.66, 119.62, 119.08, 118.91, 114.13, 107.97, 52.07, 44.79, 43.36, 40.08, 39.19, 33.83, 33.09, 21.43.

2-Acetyl-10-[(2-chloropyridin-4-yl)methyl]amino-1,2,3,4-tetrahydrobenzo[*b*][1,6]naphthyridine-8-carbonitrile (6e). Following general procedure B, 2-chloro-4-pyridinemethanamine and **5c** provided **6e**; Column chromatography using ethyl acetate/methanol, 95/5; yield 30%; ESI-HRMS (m/z) [M + H^+] calcd for C_{21} H_{19} N_5 O Cl:

392.1278, Observed: 392.1270. LC/MS Purity 99.5%, Rt = 7.22 min; ^{1}H NMR (400 MHz, $CDCl_3$): (mixture of rotamers) δ 8.42 (d, 1H, *J*=4.8 Hz), 8.25 (d, 1H, *J*=1.6 Hz), 8.01 (d, 1H, *J*=8.4 Hz), 7.76 (dd, 1H, *J*=9.2, 2.0 Hz), 7.36 (s, 1H), 7.24 (dd, 1H, *J*=4.8, 1.2 Hz), 4.76 and 4.60 (2 s, 2H), 4.72 (s, 2H, $\underline{CH_2}NH$) 4.64 (s, 1H, $CH_2\underline{NH}$), 3.94 and 3.84 (2 t, 2H, *J*=6.0 Hz), 3.24 and 3.18 (2 t, 2H, *J*=6.0 Hz), 2.22 and 2.06 (2 s, 3H); ^{13}C NMR (100 MHz, $CDCl_3$): δ 169.82, 158.68, 152.49, 151.16, 150.43, 148.90, 148.43, 130.72, 130.00, 128.87, 122.45, 120.62, 119.61, 118.74, 114.53, 108.34, 51.43, 43.32, 39.98, 33.72, 21.46.

2-Acetyl-10-[(3-chloro-4-fluorobenzyl)amino]-1,2,3,4-tetrahydrobenzo[*b*][1,6]naphthyridine-8-carbonitrile (6f). Following general procedure B, 3-chloro-4-fluoro-benzenemethanamine and **5c** provided **6f**; Column chromatography using ethyl acetate/methanol, 95/5; yield 18%. ESI-HRMS (m/z) [M + H^+] calcd for C_{22} H_{19} N_4 O F Cl: 409.1231, Observed: 409.1232; LCMS Purity 96.53%, Rt = 8.01 min; ^{1}H NMR (400 MHz, $(CD_3)_2CO$): (mixture of rotamers) δ 8.67 and 8.65 (2 s, 1H), 7.98-7.94 (m, 1H), 7.87-7.82 (m, 1H), 7.73-7.68 (m, 1H), 7.51 (s, 1H), 7.37-7.28 (m, 1H), 6.31 (s, 1H, NH), 4.89 (s, 2H), 4.84 (s, 2H), 3.92-3.86 (m, 2H), 3.19 and 3.06 (2 t, 2H, *J*=6.0 Hz), 2.17 and 2.02 (2 s, 3H); ^{13}C NMR (100 MHz, $CDCl_3$): (mixture of rotamers) δ 169.72, 168.99, 159.92, 158.43, 157.80 ($^{1}J_{C,F}$=248 Hz), 149.04, 148.87, 148.56, 135.31 ($^{4}J_{C,F}$=3 Hz), 130.79, 130.56, 130.00, 129.79, 129.62, 129.51, 128.74, 127.11 ($^{3}J_{C,F}$=7.6 Hz), 126.92 ($^{3}J_{C,F}$=7.6 Hz), 121.80, 121.62, 119.24 ($^{2}J_{C,F}$=50 Hz), 117.42 ($^{2}J_{C,F}$=21.3 Hz), 117.30 ($^{2}J_{C,F}$=21.3 Hz), 113.78, 108.26, 107.77, 52.27, 52.15, 44.75, 43.38, 40.11, 39.17, 33.83, 33.08, 21.62, 21.50.

2-Acetyl-10-[(3-chloro-5-fluoro-4-methoxybenzyl)amino]-1,2,3,4-tetrahydrobenzo[*b*][1,6]naphthyridine-8-carbonitrile (6g). Following general procedure B, 3-chloro-5-fluoro-4-methoxy-benzenemethanamine and **5c** provided **6g**; Column chromatography

using ethyl acetate/methanol, 95/5; yield 46%; ESI-HRMS (m/z) [M + H^+] calcd for C_{23} H_{21} N_4 O_2 F Cl: 439.1337, Observed: 439.1344; LC/MS Purity 96.89%, Rt = 8.11 min; ^{1}H NMR (400 MHz, $CDCl_3$): (mixture of rotamers) δ 8.29 (m, 1H), 8.04 -7.97 (2 d, 1H, *J*=8.8 Hz), 7.78 and 7.74 (1H, d, *J*=8.8 Hz and dd, *J*=8.8, 2.0 Hz), 7.19 and 7.16 (2 s, 1H), 7.02 (dd, 1H, *J*=10.8, 1.6 Hz), 4.73 and 4.59 (2 s, 3H), 4.63 and 4.56 (2 d, 2H, *J*=6.8 Hz), 4.47 (t, 1H, *J*=6.4 Hz, NH), 4.21 and 3.83 (2 t, 2H, *J*=6.4 Hz), 3.99 (s, 3H), 3.22 and 3.17 (2 t, 2H, *J*=5.6 Hz), 2.22 and 2.08 (2 s, 3H). ^{13}C NMR (100 MHz, $CDCl_3$): (mixture of rotamers) δ 169.76, 157.36, 154.85, 144.15, 144.02, 134.37, 130.05, 129.54, 129.03, 128.99, 128.77, 124.23, 124.20, 124.02, 119.24, 118.87, 114.55, 114.34, 113.55, 107.92, 61.53, 61.48, 51.91, 44.79, 43.26, 40.11, 39.12, 33.46, 29.64, 21.57, 21.45.

(3-Chloro-5-fluoro-4-methoxyphenyl)methanol (8). $NaBH_4$ (52.15 mg, 1.38 mmol) was added to a solution of 3-chloro-5-fluoro-4-methoxybenzaldehyde **7** (200 mg, 1.06 mmol) in THF (5 mL). The mixture was stirred overnight at room temperature. Iced water was added to the reaction mixture, which was partitioned between Ethyl ether (20 mL) and HCl 4N (20 mL). Organic phase was washed with HCl 4N (3 x 20mL) and dried over Na_2SO_4, filtered and evaporated. Final product **8** was obtained in quantitative amount. Yield 98%; ^{1}H NMR (400 MHz, $CDCl_3$) δ 7.16 (t, 1H, *J*=1.8 Hz), 7.04 (dd, 1H, *J*=11.4, 1.8 Hz), 4.62 (s, 2H), 3.95 (2, 3H).

2-(3-Chloro-5-fluoro-4-methoxybenzyl)isoindoline-1,3-dione (9). **8** (200mg, 1.05 mmol), phthalimide (200.7 mg, 1.36 mmol), and triphenylphosphine (356 mg, 1.36 mmol) were dissolved in THF (7 mL) and DIAD (275 mg, 1.36 mmol) was added at 0 °C. The reaction mixture was stirred at room temperature for 24h. The solvent was evaporated and the residue

partitioned between ethyl ether and H_2O. Aqueous phase was extracted 3 times with Et_2O (3 x20mL) and the organic phase was collected and dried over Na_2SO_4, filtered and evaporated. The residue was purified by flash chromatography using hexane/ethyl acetate, 90/10; yield 54%; ^{1}H NMR (400 MHz, $CDCl_3$) δ 7.87-7.85 (m, 2H), 7.74-7.72 (m, 2H), 2.35 (t, 1H, *J*=2.0 Hz), 7.10 (dd, 1H, *J*=10.8, 2.4 Hz), 4.74 (s, 2H), 3.91 (s, 3H).

(3-Chloro-5-fluoro-4-methoxyphenyl)methanamine hydrochloride (10). N_2H_4 (0.47 mmol) was added to a solution of **9** (0.09 mmol) in MeOH (2mL) and the reaction was stirred to 70 °C overnight. The reaction was cooled down and H_2O was added. The organic solvent was evaporated off and HCl conc. was added. The mixture was stirred at room temperature for 1h and the resulting precipitate was filtered off. The aqueous phase was extracted with DCM (3x 10mL) and the organic phase was discarded. Then the aqueous phase was basified and extracted with DCM (3x 10mL), dried over Na_2SO_4, filtered and evaporated under reduce pressure. The residue was treated with HCl/Et_2O 2M to give **10**. Yield 73%; ^{1}H NMR (400 MHz, DMSO-d6) δ 8.46 (s, 3H, NH_3^+), 7.52-7.51 (m, 1H), 7.48 (d, 1H, *J*=2.0 Hz), 3.99 (s, 2H), 3.90 (s, 3H).

10-Chloro-1,2,3,4-tetrahydrobenzo[*b*][1,6]naphthyridine-8-carbonitrile (11). 1-chloroethyl chloroformate (1.5 equiv) was added dropwise to a solution of benzyl derivative (1 equiv) in DCE at 0 °C. The mixture was heated to reflux for 2 h. DCE was evaporated off and the residue was dissolved in MeOH and reflux for 1 h. The formation of a precipitate was observed. After the reaction mixture was cooled down to r.t., the precipitate was collected by filtration and partitioned between NaOH 1N and AcOEt and the aqueous layer was extracted twice with AcOEt. The organic layers were dried over Na_2SO_4, filtered and evaporated under reduced pressure to yield **11**. Yield 62%; ESI-MS m/z 244 $[M+1]^+$; ^{1}H NMR (400 MHz, $CDCl_3$)

δ 8.57 (d, 1H, *J*= 1.2 Hz), 8.04 (d, 1H, *J*=8.7 Hz), 7.82 (dd, 1H, *J*=8.4, 1.8 Hz), 4.28 (s, 2H), 3.30 (t, 2H, *J*= 6.0 Hz), 3.17 (t, 2H, *J*= 6.0 Hz), 1.73 (s, 1H).

Tert-butyl 10-chloro-8-cyano-3,4-dihydrobenzo[*b*][1,6]naphthyridine-2(1*H*)-carboxylate (12). Di-tert-butyl dicarbonate (3.5 mmol) was added to a solution of **11** (3.5 mmol) in DCM (10 mL) at 0 °C. The reaction was stirred at r.t. for 1 h. The reaction was washed with $NaHCO_3$ saturated solution (2x30 mL) and the organic layer was dried over Na_2SO_4, filtered and evaporated under reduced pressure to obtain **12.** Yield 94%; ESI-MS m/z 385 $[M+MeCN]^+$; ^1H NMR (400 MHz, $CDCl_3$) δ 8.60 (s, 1H), 8.09 (d, 1H, *J*=8.8 Hz), 7.85 (d, 1H, *J*=8.4 Hz), 4.85 (s, 2H), 3.85 (t, 2H, *J*=5.8 Hz), 3.22 (t, 2H, *J*=5.2 Hz),1.52 (s, 9H).

Tert-butyl 10-[(3-chloro-4-methoxybenzyl)amino]-8-cyano-3,4-dihydrobenzo[*b*][1,6]naphthyridine-2(1*H*)-carboxylate (13). Column chromatography using hexane/ethyl acetate, 30/70; yield 49%; ESI-MS m/z 479.45 $[M+H]^+$; LC/MS Purity = 99.5%, Rt= 6.75 min; ^1H NMR (400 MHz, $CDCl_3$) δ 8.33 (d, 1H, *J*=1.5 Hz), 7.94 (d, 1H, *J*=8.7 Hz), 7.70 (dd, 1H, *J*=8.7, 1.8 Hz), 7.31 (s, 1H), 7.17 (dd, 1H, *J*=8.4, 2.1 Hz), 6.90 (d, 1H, *J*=8.1 Hz), 4.60-4.55 (m, 4H), 4.36 (s, 1H), 3.89 (2, 3H), 3.75 (t, 2H, *J*=6.0 Hz), 3.12 (t, 2H, *J*=6.0 Hz), 1.47 (s, 9H); ^{13}C NMR (100 MHz, $CDCl_3$) δ 154.98, 149.03, 148.65, 131.31, 130.51, 129.59, 129.49, 126.98, 123.10, 119.10, 112.52, 107.54, 80.56, 56.19, 52.58, 33.55, 28.36.

10-((3-Chloro-4-methoxybenzyl)amino)-1,2,3,4-tetrahydrobenzo[*b*][1,6]naphthyridine-8-carbonitrile (14). A solution of Et_2O/HCl 2.0M was added dropwise to a solution of **13** (0.21 mmol) in CH_2Cl_2: 1,4-dioxane (1:2) (1.0 mL). The mixture was stirred at r.t. overnight. The reaction mixture was diluted with HCl 1N and the organic layer was discarded. The aqueous layer was then basified by using $NaHCO_3$ and extracted with DCM (3x10 mL). The organic

layers were dried over Na_2SO_4, filtered and evaporated under reduced pressure. Column chromatography using methylene chloride/methanol, 90/10; yield 20%; ESI-HRMS (m/z) [M + H^+] calcd for C_{21} H_{20} N_4 O Cl: 379.1326, Observed: 379.1338; LC/MS Purity = 97.38%, Rt= 6.62 min; ^{1}H NMR (400 MHz, $CDCl_3$) δ 8.32 (s, 1H), 7.97 (d, 1H, *J*=9.7 Hz), 7.71 (d, 1H, *J*=9.0 Hz), 7.33 (d, 1H, *J*=1.8 Hz), 7.17 (d, 1H, *J*=8.4 Hz), 6.93 (d, 1H, *J*=8.7 Hz), 4.56 (d, 2H, *J*=5.4 Hz), 4.09 (s, 1H), 3.97 (s, 2H), 3.92 (s, 3H), 3.25 (t, 2H, *J*=6.0 Hz), 3.11 (t, 2H, *J*=6.0 Hz); ^{13}C NMR (100 MHz, $CDCl_3$) δ 159.90, 154.90, 148.93, 148.60, 131.67, 130.38, 129.47, 129.43, 129.28, 126.93, 123.03, 119.58, 119.24, 116.91, 112.46, 107.26, 56.20, 52.59, 44.84, 43.34, 34.11.

1-(10-Chloro-3,4-dihydrobenzo[*b*][1,6]naphthyridin-2(1*H*)-yl)ethan-1-one (16a). Following general procedure A, 1-acetylpiperidin-4-one and **11a** provided **16a**; Column chromatography using methylene chloride/methanol, 95/5; yield 33%; ESI-MS m/z 261 $[M+H]^+$; ^{1}H NMR (300 MHz, $CDCl_3$): (mixture of rotamers) δ 8.22-8.20 (m, 1H), 8.04-8.00 (m, 1H), 7.77-7.72 (m, 1H), 7.64-7.59 (m, 1H), 5.00 and 4.87 (2 s, 2H), 4.01 and 3.88 (2 t, 2H, *J*=5.6 Hz), 3.27 and 3.21 (2 t, 2H, *J*=6.4), 2.28 and 2.26 (2 s, 3H).

1-(10-Chloro-8-methoxy-3,4-dihydrobenzo[*b*][1,6]naphthyridin-2(1*H*)-yl)ethan-1-one (16b). Following general procedure A, 1-acetylpiperidin-4-one and **11b** provided **16b**; Column chromatography using methylene chloride/methanol, 95/5; yield 24%; ESI-MS m/z 291 $[M+H]^+$; ^{1}H NMR (400 MHz, $CDCl_3$): (mixture of rotamers) δ 7.90 (d, 1H, *J*=9.2 Hz), 7.42-7.40 (m, 1H), 7.39-7.36 (m, 1H), 4.98 and 4.85 (2 s, 2H), 4.00 and 3.86 (2 t, 2H, *J*=6.0 Hz), 3.98 and 3.97 (2 s, 3H), 3.22 and 3.17 (2 t, 2H, *J*=6.0 Hz), 2.28 and 2.25 (2 s, 3H).

1-(8-Bromo-10-chloro-3,4-dihydrobenzo[*b*][1,6]naphthyridin-2(1*H*)-yl)ethan-1-one (16c). Following general procedure A, 1-acetylpiperidin-4-one and **11c** provided **16c**; Column chromatography using methylene chloride/methanol, 95/5; yield 21%; ESI-MS m/z 340 $[M+H]^+$; ^{1}H NMR (400 MHz, $CDCl_3$) (mixture of rotamers) δ 8.36 (s, 1H), 7.88-7.78 (m, 2H), 4.99 and 4.86 (2 s, 2H), 4.00 and 3.87 (2 t, 2H, *J*= 4.8 Hz), 3.24 and 3.18 (2 t, 2H, *J*= 4.8 Hz), 3.27 and 2.25 (2 s, 3H).

8-Bromo-10-chloro-2-methyl-1,2,3,4-tetrahydrobenzo[*b*][1,6]naphthyridine (16d). Following general procedure A, 1-methylpiperidin-4-one and 2-amino-5-bromobenzoic acid provided **16d**; the desired compound was purified by triturating with Et_2O. Yield 42%; ESI-MS m/z 352 $[M+MeCN]^+$; ^{1}H NMR (300 MHz, $CDCl_3$) δ 8.33 (d, 1H, *J*= 2.1 Hz), 7.86 (d, 1H, *J*= 9.0 Hz), 7.77 (dd, 1H, *J*= 9.0, 2.1 Hz), 3.99 (s, 2H), 3.34 (t, 2H, *J*= 5.7 Hz), 3.03 (t, 2H, *J*= 5.7 Hz), 2.69 (s, 3H).

1-(10-((3-Chloro-4-methoxybenzyl)amino)-3,4-dihydrobenzo[*b*][1,6]naphthyridin-2(1*H*)-yl)ethan-1-one (17a). Following general procedure B, 3-chloro-4-methoxy-benzenemethanamine and **16a** provided **17a**; Column chromatography using ethyl acetate/methanol, 80/20; yield 24%; ESI-HRMS (m/z) $[M + H^+]$ calcd for $C_{22}\ H_{23}\ N_3\ O_2\ Cl$: 396.1479, Observed: 396.1489; LCMS Purity 99.07%, Rt = 7.74 min; ^{1}H NMR (400 MHz, DMSO-d6): (mixture of rotamers) δ 8.11 (d, 1H), 7.71-7.67 (m, 1H), 7.55-7.50 (m, 1H), 7.43 and 7.380 (2 d, 1H), 7.35-7.29 (m, 1H), 7.22-7.18 (m, 1H), 7.03 and 7.98 (2 d, 1H), 6.45 (br s, 1H, NH, D_2O exchange), 4.66 and 4.58 (2 s, 2H), 4.52 (m, 2H, $\underline{CH_2}NH$), 3.75 and 3.73 (2 s, 3H), 3.70 and 3.66 (2 t, 2H, *J*=6.4 Hz), 3.99 and 2.87 (2 t, 2H, *J*=6.0 Hz), 2.04 and 1.88 (2 s, 3H); ^{13}C NMR (100 MHz, $CDCl_3$): (mixture of rotamers) δ 169.64, 169.15, 156.56, 155.34, 154.72, 154.58, 149.01, 148.62, 147.81, 147.72, 132.23, 132.14, 130.85, 129.37, 129.28, 129.19, 128.99,

128.75, 126.92, 126.73, 125.18, 124.78, 122.96, 122.70, 122.37, 121.55, 120.68, 120.36, 113.55, 112.76, 112.31, 56.21, 56.17, 52.48, 52.29, 44.87, 43.69, 40.30, 39.58, 33.66, 32.86, 21.68, 21.58.

1-[10-((3-Chloro-4-methoxybenzyl)amino)-8-methoxy-3,4-dihydrobenzo[*b*][1,6]naphthyridin-2(1*H*)-yl]ethan-1-one (17b). Following general procedure B, 3-chloro-4-methoxy-benzenemethanamine and **16b** provided **17b**; Column chromatography using ethyl acetate/methanol, 80/20; yield 20%, ESI-HRMS (m/z) [M + H^+] calcd for C_{23} H_{25} N_3 O_3 Cl: 426.1584, Observed: 426.1592; LC/MS Purity 95.93%, Rt = 8.21 min. ^{1}H NMR (400 MHz, $CDCl_3$): (mixture of rotamers) δ 7.90 and 7.86 (2 d, 1H, *J*=9.2 Hz), 7.41 and 7.37 (2 d, 1H *J*=2.0 Hz), 7.31-7.27 (dd, 1H, *J*=9.6, 2.8 Hz), 7.23 (dd, 1H, *J*=8.0, 2.4 Hz), 7.15 and 7.11 (2 d, 1H, *J*=2.8 Hz), 6.92-6.87 (m, 1H), 4.74 and 4.58 (2 s, 2H), 4.52 and 4.45 (s, 1.5H), 3.90 (s, 4H, OCH_3 and NH), 3.80 (t, 2H, *J*=6.4 Hz), 3.84 and 3.75 (2 s, 3H), 3.18 and 3.13 (2 t, 2H, *J*=6.0 Hz), 2.21 and 2.08 (s, 3H); ^{13}C NMR (100 MHz, $CDCl_3$): (mixture of rotamers) δ 169.67, 169.15, 157.07, 156.73, 154.69, 154.50, 153.92, 152.73, 148.24, 147.61, 143.74, 143.59, 132.48, 130.75, 130.39, 129.24, 129.17, 126.70, 122.99, 122.70, 121.75, 121.48, 121.41, 114.78, 114.08, 112.29, 101.19, 100.54, 56.19, 55.44, 55.32, 52.16, 51.81, 44.80, 43.77, 40.30, 39.61, 33.33, 32.53, 21.65, 21.54.

1-[8-Bromo-10-((3-chloro-4-methoxybenzyl)amino)-3,4-dihydrobenzo[*b*][1,6]naphthyridin-2(1*H*)-yl]ethan-1-one (17c). Following general procedure B, 3-chloro-4-methoxy-benzenemethanamine and **16c** provided **17c**; Column chromatography using methylene chloride/methanol, 95/5; yield 42%; ESI-HRMS (m/z) [M + H^+] calcd for C_{22} H_{22} N_3 O_2 Cl Br: 474.0584, Observed: 474.0587; LC/MS Purity = 97.86%, Rt= 5.8 min; ^{1}H NMR (400 MHz, $CDCl_3$): (mixture of rotamers) δ 8.09 and 8.05 (2 d, 1H, *J*=1.6 Hz), 7.86-7.82

(m, 1H), 7.73-7.67 (m, 1H), 7.37 and 7.32 (2 d, 1H, *J*=2.0 Hz), 7.21 and 7.12 (2 dd, 1H, *J*=8.8, 0.75 Hz), 6.94-6.90 (m, 1H), 4.71 and 4.48 (2 s, 2H), 4.56 (s, 2H), 3.91 (s, 3H), 3.8 (t, 2H, *J*=6.0 Hz), 3.19 and 3.13 (2 t, 2H, *J*=6.0 Hz), 2.21 and 2.05 (2 s, 3H); ^{13}C NMR (100 MHz, $CDCl_3$): (mixture of rotamers) δ 169.62, 169.08, 157.05, 155.79, 154.85, 154.71, 148.08, 147.69, 146.48, 146.45, 132.70, 132.48, 131.98, 131.85, 131.07, 130.79, 129.45, 129.29, 126.98, 126.74, 124.32, 125.09, 123.10, 122.80, 122.02, 121.64, 118.90, 118.38, 114.44, 113.67, 112.39, 112.36, 56.22, 56.18, 52.52, 52.35, 44.76, 43.56, 40.21, 33.65, 32.83, 21.59, 21.51.

8-Bromo-N-(3-chloro-4-methoxybenzyl)-2-methyl-1,2,3,4-tetrahydrobenzo[*b*][1,6]naphthyridin-10-amine (17d). Following general procedure B, 3-chloro-4-methoxy-benzenemethanamine and **16b** provided **17b**; Column chromatography using ethyl acetate/methanol, 80/20; yield 38%; ESI-HRMS (m/z) [M + H^+] calcd for C_{21} H_{22} N_3 O Cl Br: 446.0557, Observed: 446.0504; LC/MS Purity = 96.43%, Rt= 7.1 min; ^{1}H NMR (400 MHz, $CDCl_3$) δ 8.04 (d, 1H, *J*= 2.4 Hz), 7.80 (d, 1H, *J*= 8.8 Hz), 7.65 (dd, 1H, *J*=9.0, 2.4 Hz), 7.38 (d, 1H, *J*= 2.0 Hz), 7.17 (dd, 1H, *J*=8.4, 2.0 Hz), 6.92 (d, 1H, *J*= 8.8 Hz), 4.47 (s, 2H), 3.92 (s, 4H, OCH_3 and NH), 3.54 (s, 2H), 3.18 (t, 2H, *J*= 6.0 Hz), 2.812 (t, 2H, *J*= 6.0 Hz), 2.50 (s, 3H); ^{13}C NMR (100 MHz, $CDCl_3$) δ 156.49, 154.64, 147.65, 146.41, 132.22, 132.05, 130.80, 129.50, 126.98, 124.82, 122.75, 121.65, 118.01, 115.97, 112.26, 56.19, 54.43, 52.378, 52.34, 46.22, 33.54.

2,4-Dioxo-1,4-dihydro-2H-benzo[*d*][1,3]oxazine-6-carbonitrile (19a). Following general procedure C, **18a** (1.5 g, 8.25 mmol) and triphosgene (0.914 g, 3.08 mmol) provided **19a**; Yield 87%; ESI-MS m/z 187 [M-H]$^-$; ^{1}H NMR (400 MHz, DMSO-d_6) δ 12.15 (s, 1H), 8.38 (d, 1H, *J*=1.6 Hz), 8.11 (dd, 1H, *J*=8.8, 1.6 Hz), 7.25 (d, 1H, *J*=8.4 Hz).

6-Methoxy-2H-benzo[*d*][1,3]oxazine-2,4(1*H*)-dione (19b). Following general procedure C, **18b** (0.5 g, 3.0 mmol) and triphosgene (0.297 g, 1.0 mmol) provided **19b**; Yield 88%; ^{1}H NMR (400 MHz, DMSO-d_6) δ 11.61 (s, 1H), 7.38 (dd, 1H, *J*=8.4, 2.8 Hz), 7.34 (d, 1H, *J*=2.4 Hz), 7.11 (d, 1H, *J*=8.4 Hz), 3.80 (s, 3H).

6-(Trifluoromethyl)-2H-benzo[*d*][1,3]oxazine-2,4(1*H*)-dione (19c). Following general procedure C, **18c** (0.8 g, 3.9 mmol) and triphosgene (0.386 g, 1.3 mmol) provided **19c**; Yield 84%; ESI-MS m/z 230 $[M-H]^-$; ^{1}H NMR (400 MHz, DMSO-d_6) δ 12.09 (s, 1H), 8.14 (d, 1H, *J*=1.2 Hz), 8.07 (dd, 1H, *J*=8.8, 1.6 Hz), 7.32 (d, 1H, *J*=8.8 Hz).

Methyl 6-cyano-2-methyl-4-oxo-1,4-dihydroquinoline-3-carboxylate (20a). Following general procedure D, **19a** (1.0 g, 5.32 mmol) and methyl acetoacetate (0.740 g, 6.38 mmol) provided **20a**; Yield 49%; ESI-MS m/z 243 $[M+H]^+$; ^{1}H NMR (400 MHz, DMSO-d_6) δ 12.25 (s, 1H), 8.39 (d, 1H, *J*=2.0 Hz), 8.01 (dd, 1H, *J*=8.8, 2.0 Hz), 7.66 (d, 1H, *J*=8.8 Hz), 3.70 (s, 3H), 2.41 (s, 3H).

Methyl 6-methoxy-2-methyl-4-oxo-1,4-dihydroquinoline-3-carboxylate (20b). Following general procedure D, **19b** (0.502 g, 2.6 mmol) and methyl acetoacetate (0.360 g, 3.1 mmol) provided **20b**; Yield 70%; ESI-MS m/z 192 $[M-H]^-$; ^{1}H NMR (400 MHz, DMSO-d_6) δ 11.61 (s, 1H), 7.38 (dd, 1H, *J*=8.4, 2.8 Hz), 7.34 (d, 1H, *J*=2.4 Hz), 7.11 (d, 1H, *J*=8.4 Hz), 3.80 (s, 3H).

Methyl 2-methyl-4-oxo-6-(trifluoromethyl)-1,4-dihydroquinoline-3-carboxylate (20c). Following general procedure D, **19c** (0.6 g, 2.6 mmol) and methyl acetoacetate (0.360 g, 3.1 mmol) provided **20c**; Yield 62%; ESI-MS m/z 286 $[M+H]^+$; ^{1}H NMR (400 MHz, $CDOD_3$) δ 8.52 (s, 1H), 7.92 (d, 1H, J=8.8 Hz), 7.70 (d, 1H, J=8.8 Hz), 3.89 (s, 3H), 2.54 (s, 3H).

Methyl 2-methyl-4-oxo-1,4-dihydroquinoline-3-carboxylate (20d). Following general procedure D, isatoic anhydride **19d** (1.0 g, 6.13 mmol) and methyl acetoacetate (0.854 g, 7.35

mmol) provided **20d**; Yield 65%; ESI-MS m/z 218 $[M+H]^+$; ^{1}H NMR (400 MHz, DMSO-d_6) δ 11.88 (s, 1H), 8.05 (d, 1H, *J*=8.0 Hz), 7.69-7.65 (m, 1H), 7.53 (d, 1H, *J*=8.4 Hz), 7.36 (m, 1H), 3.76 (s, 3H), 2.39 (s, 3H).

Methyl 6-chloro-2-methyl-4-oxo-1,4-dihydroquinoline-3-carboxylate (20e). Following general procedure D, 5-chloroisatoic anhydride **19e** (1.5 g, 7.6 mmol) and methyl acetoacetate (1.05 g, 9.1 mmol) provided **20d**; Yield 64%; ESI-MS m/z 252 $[M+H]^+$; ^{1}H NMR (400 MHz, DMSO-d_6) δ 12.07 (s, 1H), 7.98 (d, 1H, *J*=2.4 Hz), 7.71 (dd, 1H, *J*=8.4, 2.4 Hz), 7.57 (d, 1H, *J*=8.8 Hz), 3.76 (s, 3H), 2.39 (s, 3H).

Methyl 4-chloro-6-cyano-2-methylquinoline-3-carboxylate (21a). Following general procedure E, **20a** (0.485 g, 2.0 mmol) in $POCl_3$ (4.0 mL) provided **21a**; Yield 19%; ESI-MS m/z 261 $[M+H]^+$; ^{1}H NMR (400 MHz, $CDCl_3$) δ 8.61 (d, 1H, *J*=2.0 Hz), 8.12 (d, 1H, *J*=8.8 Hz), 7.92 (dd, 1H, *J*=8.4, 1.6 Hz), 4.05 (s, 3H), 2.75 (s, 3H).

Methyl 4-chloro-6-methoxy-2-methylquinoline-3-carboxylate (21b). Following general procedure E, **20b** (0.400 g, 1.6 mmol) in $POCl_3$ (3.0 mL) provided **21b**; Yield 93%; ESI-MS m/z 266 $[M+H]^+$; ^{1}H NMR (400 MHz, $CDCl_3$) δ 7.93 (d, 1H, *J*=9.6 Hz), 7.43-7.41 (m, 2H), 4.03 (s, 3H), 3.97 (s, 3H), 2.67 (s, 3H).

Methyl 4-chloro-2-methyl-6-(trifluoromethyl)quinoline-3-carboxylate (21c). Following general procedure E, **20c** (0.456 g, 1.6 mmol) in $POCl_3$ (1.0 mL) provided **21c**; Yield 51%; ESI-MS m/z 304 $[M+H]^+$; ^{1}H NMR (400 MHz, $CDCl_3$) δ 8.53 (s, 1H), 8.15 (d, 1H, *J*=8.8 Hz), 7.95 (dd, 1H, *J*=8.8, 1.6 Hz), 4.05 (s, 3H), 2.75 (s, 3H).

Methyl 4-chloro-2-methylquinoline-3-carboxylate (21d). Following general procedure E, **20d** (0.487 g, 3.9 mmol) in $POCl_3$ (3.0 mL) provided **21d**; Yield 90%; ESI-MS m/z 236 $[M+H]^+$;

^{1}H NMR (400 MHz, $CDCl_3$) δ 8.4 (d, 1H, *J*=8.4 Hz), 8.03 (d, 1H, *J*=8.4 Hz), 7.79 (td, 1H, J_1=1.2, J_2=7.2), 7.63 (t, 1H, *J*=8.4), 4.04 (s, 3H), 2.72 (s, 3H).

Methyl 4,6-dichloro-2-methylquinoline-3-carboxylate (21e). Following general procedure E, **20e** (0.755 g, 3.0 mmol) in $POCl_3$ (4.0 mL) provided **21e**; Yield 91%; ESI-MS m/z 311 $[M+MeCN]^+$; ^{1}H NMR (400 MHz, DMSO-d_6) δ 8.21 (d, 1H, *J*=2.4 Hz), 8.08 (d, 1H, *J*=9.2 Hz), 7.95 (dd, 1H, *J*=8.8, 2.4 Hz), 4.01 (s, 3H), 2.63 (s, 3H).

Methyl 2-(bromomethyl)-4-chloro-6-cyanoquinoline-3-carboxylate (22a). Following general procedure F, **21a** (0.08 g, 0.3 mmol), *N*-bromosuccinimide (0.08 g, 0.46 mmol) and 2,2'-Azobis(2-methylpropionitrile) (0.01 g, 0.06 mmol) provided **22a**; Purification by column chromatography using hexane/ethyl acetate, 90/10; yield 39%; ESI-MS m/z 341 $[M+1]^+$.

Methyl 2-(bromomethyl)-4-chloro-6-methoxyquinoline-3-carboxylate (22b). Following general procedure F, **21b** (0.390 g, 1.47 mmol), *N*-bromosuccinimide (0.392 g, 2.20 mmol) and 2,2'-Azobis(2-methylpropionitrile) (0.048 g, 0.3 mmol) provided **22b**; Purification by column chromatography using hexane/ethyl acetate, 90/10; yield 16%; ESI-MS m/z 346 $[M+1]^+$; ^{1}H NMR (400 MHz, $CDCl_3$) δ 7.98 (d, 1H, *J*=10.4 Hz), 7.47-7.44 (m, 2H), 4.77 (s, 2H), 4.07 (s, 3H), 3.99 (s, 3H).

Methyl 2-(bromomethyl)-4-chloro-6-(trifluoromethyl)quinoline-3-carboxylate (22c). Following general procedure F, **21c** (0.130 g, 0.43 mmol), *N*-bromosuccinimide (0.115 g, 0.64 mmol) and 2,2'-Azobis(2-methylpropionitrile) (0.014 g, 0.09 mmol) provided **22c**; Purification by column chromatography using hexane/ethyl acetate, 90/10; yield 55%; ESI-MS m/z 384 $[M+1]^+$; ^{1}H NMR (400 MHz, $CDCl_3$) δ 8.58 (d, 1H, *J*=1.2 Hz), 8.22 (d, 1H, *J*=8.8 Hz), 8.01 (dd, 1H, *J*=8.8, 2.0 Hz), 4.77 (s, 2H), 4.06 (s, 3H).

Methyl 2-(bromomethyl)-4-chloroquinoline-3-carboxylate (22d). Following general procedure F, **21d** (0.810 g, 3.44 mmol), *N*-bromosuccinimide (0.918 g, 5.15 mmol) and 2,2'-Azobis(2-methylpropionitrile) (0.113 g, 0.7 mmol) provided **22d**; Purification by **c**olumn chromatography using dichloromethane; yield 57%; ESI-MS m/z 315 $[M+1]^+$; ^{1}H NMR (400 MHz, $CDCl_3$) δ 8.28 (dd, 1H, *J*=8.0, 1.2 Hz), 8.09 (d, 1H, *J*=8.0 Hz), 7.86-7.82 (m, 1H), 7.73-7.68 (m, 1H), 4.80 (s, 2H), 4.08 (s, 3H).

Methyl 2-(bromomethyl)-4,6-dichloroquinoline-3-carboxylate (22e). Following general procedure F, **21e** (0.400 g, 1.5 mmol), *N*-bromosuccinimide (0.405 g, 2.25 mmol) and 2,2'-Azobis(2-methylpropionitrile) (0.049 g, 0.3 mmol) provided **22e**; Purification by column chromatography using hexane/ethyl acetate, 60/40; yield 35%; ESI-MS m/z 350 $[M+H]^+$; ^{1}H NMR (400 MHz, $CDCl_3$) δ 8.26 (d, 1H, *J*=2.0 Hz), 8.04 (d, 1H, *J*=8.4 Hz), 7.78 (dd, 1H, *J*=8.8, 2.4 Hz), 4.78 (s, 2H), 4.08 (s, 3H).

9-Chloro-2-ethyl-1-oxo-2,3-dihydro-1*H*-pyrrolo[3,4-*b*]quinoline-7-carbonitrile (23a). Following general procedure G, **22a** (0.052 g, 0.15 mmol) and $EtNH_2$ (0.230 mL, 0.46 mmol) provided **23a**; Purification by column chromatography using hexane/ethyl acetate, 30/70; yield 25%; ESI-MS m/z 272 $[M+1]^+$; ^{1}H NMR (400 MHz, $CDCl_3$) δ 8.84 (d, 1H, *J*=2.0 Hz), 8.23 (d, 1H, *J*=1.4 Hz), 7.99 (dd, 1H, *J*=8.8, 1.6 Hz) , 4.57 (s, 2H), 3.78 (q, 2H, *J*=7.2 Hz), 1.35 (t, 3H, *J*=6.8 Hz).

9-Chloro-2-ethyl-7-methoxy-2,3-dihydro-1*H*-pyrrolo[3,4-*b*]quinolin-1-one (23b). Following general procedure G, **22b** (0.060 g, 0.17 mmol) and $EtNH_2$ (0.260 mL, 0.52 mmol) provided **23b**; Purification by column chromatography using hexane/ethyl acetate, 30/70; yield 72%; ESI-MS m/z 277 $[M+1]^+$; ^{1}H NMR (400 MHz, $CDCl_3$) δ 8.01 (d, 1H, *J*=8.8 Hz), 7.64 (d,

1H, *J*=2.8 Hz), 7.50 (dd, 1H, *J*=9.6, 2.8 Hz), 4.49 (s, 2H), 4.01 (s, 3H), 3.76 (q, 2H, *J*=7.2 Hz), 1.33 (t, 3H, *J*=7.2 Hz).

9-Chloro-2-ethyl-7-(trifluoromethyl)-2,3-dihydro-1*H*-pyrrolo[3,4-*b*]quinolin-1-one (23c). Following general procedure G, **22c** (0.080 g, 0.21 mmol) and $EtNH_2$ (0.315 mL, 0.63 mmol) provided **23c**; Purification by column chromatography using hexane/ethyl acetate, 50/50; yield 45%; ESI-MS m/z 315 $[M+1]^+$; ^1H NMR (400 MHz, $CDCl_3$) δ 8.76 (s, 1H), 8.26 (d, 1H, *J*=8.8 Hz), 8.03 (dd, 1H, *J*=8.8, 2.0 Hz) , 4.57 (s, 2H), 3.79 (q, 2H, *J*=6.8 Hz), 1.35 (t, 3H, *J*=6.8 Hz).

9-Chloro-2-ethyl-2,3-dihydro-1*H*-pyrrolo[3,4-*b*]quinolin-1-one (23d). Following general procedure G, **22d** (0.080 g, 0.26 mmol) and $EtNH_2$ (0.382 mL, 0.76 mmol) provided **23d**; Purification by column chromatography using hexane/ethyl acetate, 30/70; yield 84%; ESI-MS m/z 247 $[M+1]^+$; ^1H NMR (400 MHz, $CDCl_3$) δ 8.46 (d, 1H, *J*=8.4 Hz), 8.13 (d, 1H, *J*=8.4 Hz), 7.87 (m, 1H), 7.72 (m, 1H), 4.53 (s, 2H), 3.77 (q, 2H, *J*=7.2 Hz), 1.34 (t, 3H, *J*=7.2 Hz).

7,9-Dichloro-2-ethyl-2,3-dihydro-1*H*-pyrrolo[3,4-*b*]quinolin-1-one (23e). Following general procedure G, **22e** (0.144 g, 0.41 mmol) and $EtNH_2$ (0.619 mL, 1.24 mmol) provided **23d**; Purification by column chromatography using hexane/ethyl acetate, 30/70; yield 54%; ESI-MS m/z 281 $[M+1]^+$; ^1H NMR (400 MHz, $CDCl_3$) δ 8.43 (d, 1H, *J*=2.0 Hz), 8.07 (d, 1H, *J*=8.8 Hz), 7.79 (dd, 1H, *J*=8.8, 2.4 Hz), 4.52 (s, 2H), 3.78 (q, 2H, *J*=7.6 Hz), 1.33 (t, 3H, *J*=7.6 Hz).

2-(Tert-butyl)-9-chloro-2,3-dihydro-1*H*-pyrrolo[3,4-*b*]quinolin-1-one (23f). Following general procedure G, **22e** (0.100 g, 0.32 mmol) and *tert*-butylamine (0.101 mL, 0.95 mmol) provided **23f**; Purification by column chromatography using hexane/ethyl acetate, 30/70; yield 28%; ESI-MS m/z 275 $[M+1]^+$; ^1H NMR (400 MHz, $CDCl_3$) δ 8.46 (dd, 1H, *J*=8.4, 1.2 Hz), 8.12 (d, 1H, *J*=8.8 Hz), 7.88-7.84 (m, 1H), 7.73-7.69 (m, 1H), 4.60 (s, 2H), 1.63 (s, 9H).

9-((3-Chloro-4-methoxybenzyl)amino)-2-ethyl-1-oxo-2,3-dihydro-1*H*-pyrrolo[3,4-*b*]quinoline-7-carbonitrile (24a). Following general procedure H, **23a** (0.01 g, 0.037 mmol), 3-chloro-4-methoxybenzylamine hydrochloride (0.012 g, 0.055 mmol) and DIPEA (0.029 g, 0.22 mmol) provided **24a**; yield 79%; ESI-HRMS (m/z) [M + H^+] calcd for $C_{22}H_{20}N_4O_2Cl$: 407.1275, Observed: 407.1264; LCMS Purity 95.4%, R_f = 10.7 min; ^{1}H NMR (400 MHz, $CDCl_3$) δ 8.58 (t, 1H, *J*=6.0 Hz), 8.53 (d, 1H, *J*=1.6 Hz), 7.94 (d, 1H, *J*=9.2 Hz), 7.75 (dd, 1H, *J*=8.4, 1.6 Hz), 7.42 (d, 1H, *J*=1.6 Hz), 7.30 (dd, 1H, *J*=8.4, 2.4 Hz), 6.96 (d, 1H, *J*=8.4 Hz), 4.93 (d, 2H, *J*=5.6 Hz), 4.38 (s, 2H), 3.89 (s, 3H), 3.63 (q, 2H, *J*=7.2 Hz), 1.27 (t, 3H, *J*=7.2 Hz). ^{13}C NMR (100 MHz, $CDCl_3$): δ 168.73, 163.90, 155.00, 153.37, 151.20, 132.19, 131.26, 130.88, 129.84, 129.17, 126.54, 123.28, 118.73, 118.13, 112.65, 106.89, 105.80, 56.18, 50.68, 50.02, 36.56, 13.43.

9-((3-Chloro-4-methoxybenzyl)amino)-2-ethyl-7-methoxy-2,3-dihydro-1*H*-pyrrolo[3,4-*b*]quinolin-1-one (24b). Following general procedure H, **23b** (0.03 g, 0.11 mmol), 3-chloro-4-methoxybenzylamine hydrochloride (0.034 g, 0.16 mmol) and DIPEA (0.085 g, 0.66 mmol) provided **24b**; yield 55%; ESI-HRMS (m/z) [M + H^+] calcd for $C_{22}H_{23}N_3O_3Cl$: 412.1428, Observed: 412.1429; LCMS Purity 98.5%, R_f = 8.8 min; ^{1}H NMR (400 MHz, $CDCl_3$) δ 8.14 (t, 1H, *J*=6.4 Hz), 7.85 (d, 1H, *J*=9.6 Hz), 7.48 (d, 1H, *J*=2.4 Hz), 7.37-7.29 (m, 3H), 6.95 (d, 1H, *J*=8.8 Hz), 4.95 (d, 2H, *J*=6.8 Hz), 4.38 (s, 2H), 3.90 (s, 3H), 3.66 (q, 2H, *J*=7.2 Hz), 3.59 (s, 3H), 1.28 (t, 3H, *J*=7.2 Hz); ^{13}C NMR (100 MHz, $CDCl_3$): δ 169.39, 159.13, 155.70, 154.45, 151.42, 147.37, 131.83, 130.69, 128.63, 125.97, 122.89, 122.39, 119.22, 112.40, 105.64, 104.52, 56.19, 55.22, 50.45, 49.43, 36.50, 13.45.

9-((3-Chloro-4-methoxybenzyl)amino)-2-ethyl-7-(trifluoromethyl)-2,3-dihydro-1*H*-pyrrolo[3,4-*b*]quinolin-1-one (24c). Following general procedure H, **23c** (0.03 g, 0.1 mmol), 3-

chloro-4-methoxybenzylamine hydrochloride (0.030 g, 0.14 mmol) and DIPEA (0.074 g, 0.57 mmol) provided **24c**; yield 99%; ESI-HRMS (m/z) [M + H^+] calcd for C_{22} H_{20} N_3 O_2 Cl F_3: 450.1196, Observed: 450.1189; LCMS Purity 95.0%, R_f = 11.5 min; ^{1}H NMR (400 MHz, $CDCl_3$) δ 8.58 (t, 1H, *J*=6.0 Hz), 8.46 (s, 1H), 8.0 (d, 1H, *J*=8.8 Hz), 7.80 (dd, 1H, *J*=9.2, 2.0 Hz), 7.45 (d, 1H, *J*=2.0 Hz), 7.32 (dd, 1H, *J*=8.4, 2.4 Hz), 6.95 (d, 1H, *J*=8.0 Hz), 4.95 (d, 2H, *J*=6.0 Hz), 4.41 (s, 2H), 3.90 (s, 3H), 3.67 (q, 2H, *J*=7.2 Hz), 1.3 (t, 3H, *J*=7.2 Hz); ^{13}C NMR (100 MHz, $CDCl_3$): δ 169.01, 163.19, 154.81, 153.27, 151.89, 130.55, 130.34, 129.06, 126.40, 126.35 (J_{CF}=3.0 Hz), 125.24 (J_{CF}=32.0 Hz), 123.99 (J_{CF}=270.1 Hz), 123.78 (J_{CF}=4.5 Hz), 123.14, 117.52, 112.53, 105.59, 56.17, 50.65, 49.79, 36.53, 13.44.

9-((3-Chloro-4-methoxybenzyl)amino)-2-ethyl-2,3-dihydro-1*H*-pyrrolo[3,4-*b*]quinolin-1-one (24d). Following general procedure H, **23d** (0.054 g, 0.22 mmol), 3-chloro-4-methoxybenzylamine hydrochloride (0.068 g, 0.33 mmol) and DIPEA (0.170 g, 1.31 mmol) provided **24d**; yield 63%; ESI-HRMS (m/z) [M + H^+] calcd for C_{21} H_{21} N_3 O_2 Cl: 382.1322, Observed: 382.1334 LCMS Purity 99.5%, R_f = 8.5 min ^{1}H NMR (400 MHz, $CDCl_3$) δ 8.26 (t, 1H, *J*=6.0 Hz), 8.14 (dd, 1H, *J*=8.0, 1.2 Hz), 7.94 (dd, 1H, *J*=8.8, 1.2 Hz), 7.68-7.64 (m, 1H), 7.45 (d, 1H, *J*=2.4 Hz), 7.33-7.29 (m, 1H), 6.95 (d, 1H, *J*=8.4 Hz), 4.98 (d, 2H, *J*=5.6 Hz), 4.39 (s, 2H), 3.90 (s, 3H), 3.65 (q, 2H, *J*=7.6 Hz), 1.29 (t, 3H, *J*=7.6 Hz); ^{13}C NMR (100 MHz, $CDCl_3$): δ 169.38, 161.26, 154.59, 151.81131.19, 130.70, 129.50, 129.06, 126.35, 125.41, 123.81, 122.90, 118.68, 112.48, 104.93, 56.15, 50.56, 50.00, 36.47, 13.44.

7-Chloro-9-((3-chloro-4-methoxybenzyl)amino)-2-ethyl-2,3-dihydro-1*H*-pyrrolo[3,4-*b*]quinolin-1-one (24e). Following general procedure H, **23e** (0.050 g, 0.18 mmol), 3-chloro-4-methoxybenzylamine hydrochloride (0.056 g, 0.27 mmol) and DIPEA (0.140 g, 1.08 mmol) provided **24e**; yield 85%; ESI-HRMS (m/z) [M + H^+] calcd for C_{21} H_{20} N_3 O_2 Cl_2: 416.0933,

Observed: 416.0930; LCMS Purity 99.5%, R_f= 10.2 min; ^{1}H NMR (400 MHz, $CDCl_3$) δ 8.29 (t, 1H, *J*=5.6 Hz), 8.14 (d, 1H, *J*=2.0 Hz), 7.86 (d, 1H, *J*=9.2 Hz), 7.58 (dd, 1H, *J*=9.2, 2.0 Hz), 7.45 (d, 1H, *J*=1.2 Hz), 7.32 (d, 1H, *J*=8.8 Hz), 6.95 (d, 1H, *J*=8.4 Hz), 4.93 (d, 2H, *J*=6.0 Hz), 4.37 (s, 2H), 3.91 (s, 3H), 3.64 (q, 2H, *J*=7.6 Hz), 1.28 (t, 3H, *J*=7.2 Hz); ^{13}C NMR (100 MHz, $CDCl_3$): δ 169.06, 161.48, 154.73, 150.79, 150.29, 131.24, 130.95, 130.75, 129.24, 129.22, 126.53, 124.65, 123.01, 119.21, 112.50, 105.36, 56.15, 50.52, 49.90, 36.51, 13.43.

2-(Tert-butyl)-9-((3-chloro-4-methoxybenzyl)amino)-2,3-dihydro-1*H*-pyrrolo[3,4-*b*]quinolin-1-one (24f). Following general procedure H, **23f** (0.121 g, 0.44 mmol), 3-chloro-4-methoxybenzylamine hydrochloride (0.137 g, 0.66 mmol) and DIPEA (0.341 g, 2.64 mmol) provided **24f**; yield 44%; ESI-HRMS (m/z) [M + H^+] calcd for C_{18} H_{25} N_5 O_4 Cl: 410.1595, Observed: 410.1620; LCMS Purity 99.2%, R_f= 9.5 min; ^{1}H NMR (400 MHz, $CDCl_3$) δ 8.53 (t, 1H, *J*=6.4 Hz, CH_2<u>NH</u>), 8.10 (d, 1H, *J*=8.4 Hz), 7.92 (d, 1H, *J*=8.0 Hz), 7.63 (t, 1H, *J*=7.6 Hz), 7.45 (d, 1H, *J*=2.0 Hz), 7.33-7.25 (m, 2H), 6.94 (d, 1H, *J*=8.8 Hz), 4.94 (d, 2H, <u>CH_2</u>NH, *J*=6.8 Hz), 4.46 (s, 2H), 3.91 (s, 3H), 1.57 (s, 9H); ^{13}C NMR (100 MHz, $CDCl_3$): δ 170.53, 160.84, 154.51, 152.02, 151.91, 131.32, 130.52, 129.44, 128.90, 126.23, 125.47, 123.54, 122.90, 118.65, 112.42, 106.16, 56.15, 54.39, 49.86, 49.76, 28.19.

PDE Enzymatic activity. Experiments were performed by BPS Bioscience, Inc. The enzymatic reactions were conducted at room temperature for 60 minutes in a 50 µl volume containing PDE assay buffer, 100 nM FAM-cGMP or FAM-cAMP substrate, 0.1-0.45 ng PDE5 or 22.5-250 ng PDE6, and the test compound. After the enzymatic reaction, 100 µl of a binding solution (1:100 dilution of the binding agent with the binding agent diluent) was added to each sample. After 60 minutes at room temperature fluorescence intensity was measured at an

excitation of 485 nm and an emission of 528 nm using a Tecan Infinite M1000 microplate reader. PDE activity assays were performed in duplicate at each concentration. Fluorescence intensity is converted to fluorescence polarization using the Tecan Magellan6 software. The fluorescence polarization data were analyzed using the computer software, Graphpad Prism. The fluorescence polarization (FPt) in absence of the compound in each data set was defined as 100% activity. In the absence of PDE and the compound, the value of fluorescent polarization (FPb) in each data set was defined as 0% activity. The percent activity in the presence of the compound was calculated according to the following equation: % activity = (FP-FPb)/(FPt-FPb)×100%, where FP= the fluorescence polarization in the presence of the compound. The values of % activity versus a series of compound concentrations were then plotted using non-linear regression analysis of Sigmoidal dose-response curve generated with the equation Y=B+(T-B)/1+$10^{((\text{LogEC50-X})\times\text{Hill Slope})}$, where Y=percent activity, B=minimum percent activity, T=maximum percent activity, X= logarithm of compound and Hill Slope=slope factor or Hill coefficient. The IC_{50} value was determined by the concentration causing a half-maximal percent activity. Standard errors were calculated using the following equation SE=IC50(mean)-IC50(Low)*$\frac{SE(Log\ IC50)}{Log\ IC50(mean)-LogIC50(Low)}$

Computational Methods. All calculations were performed using the Schrodinger molecular modeling suite (version 2016-2). The protein structure used for PDE5A1 was obtained from the Protein Data Bank (3TGG.pdb)[33] and prepared using the Protein Preparation Wizard.[34] In this step, force field atom types and bond orders are assigned, missing atoms added, tautomer/ionization states are assigned, water orientations are sampled, Asn, Gln and His residues are flipped to optimize the hydrogen bond network, and a constrained energy

minimization is performed. The water molecules present in the crystal structures were conserved. Of note, only a few were present in the targeted binding site and were located at its periphery.

In silico docking. Compounds 6c and 24a were docked into the cGMP binding site of PDE5A1 using Glide.[35, 36] In both cases, the docking region (grid) was centered on the position of the crystal ligand (in 3TGG.pdb), that occupies the targeted region in the cGMP binding site. Default box sizes were used. Glide docks flexible ligands into a rigid receptor structure by sampling of the conformational, positional and orientational degrees of freedom of the ligand. No constraint was used for the docking calculations. The poses obtained were further refined using minimization of the binding pocket around the docked ligands.

WaterMap calculations. WaterMap is a molecular dynamics-based method that predicts the locations and thermodynamic properties (entropy, enthalpy and free energy) of explicit water molecules in a region of interest around a protein. The theoretical basis for the method as well as the specific computational algorithms used are fully described elsewhere.[26, 27] In brief, WaterMap clusters and makes the statistical analysis of the water molecules around the site of interest from many frames of a molecular dynamics simulation. Regions of high water density (high occupancy) are identified as "hydration sites", and their corresponding enthalpies and entropies are computed relatives to bulk solvent using inhomogeneous solvation theory.[37, 38] I n the work presented here, we ran WaterMap in the binding pocket in the absence of any ligand.

Kinetic solubility assay. Experiments were performed by Cyprotex US, LLC. Serial dilutions of each compound were prepared in DMSO at 100x the final concentration. Test compound solutions were diluted 100-fold into buffer in a 96-well plate and mixed. After 18 h

incubation at 37°C, the presence of precipitate was then detected by turbidity (absorbance at 540 nm). Precipitate forms when maximum aqueous solubility levels were reached. An absorbance value greater than 'mean + 3x standard deviation of the blank (after subtracting the background) was indicative of turbidity. For brightly colored compounds, a visual inspection of the plate was performed to verify the solubility limit determined by UV absorbance. The solubility limit was reported as the highest experimental concentration with no evidence of turbidity. Reserpine and tamoxifen were used as low solubility control, verapamil was used as high solubility control.

Microsomal stability. Experiments were performed by Absorption Systems. Human liver microsomes were purchased from XenoTech. The test compounds were added into the reaction mixture at a final concentration of 1 μM. An aliquot of the reaction mixture (without cofactor) was incubated in a shaking water bath at 37°C for 3 minutes. The control compound, testosterone, was run simultaneously with the test compounds in a separate reaction. The reaction was initiated by the addition of cofactor, and the mixture was then incubated in a shaking water bath at 37°C. Aliquots (100 μL) were withdrawn at 0, 10, 20, 30, and 60 minutes for the test compound and 0, 10, 30, and 60 minutes for testosterone. Test compound and testosterone samples were immediately combined with 400 μL of ice-cold 50/50 acetonitrile/dH_2O containing 0.1% formic acid and internal standard to terminate the reaction. The samples were then mixed and centrifuged to precipitate microsomal proteins. Samples for test compounds were analyzed by LC-HRAMS for disappearance of test compound and appearance of metabolites. All the remaining samples were assayed by LC-MS/MS using electrospray ionization. Analytical conditions are outlined in Appendix 1. The peak area response ratio (PARR) to internal standard was compared to the PARR at time 0 to determine the

percent of test compound or positive control remaining at each time point. Half-lives were calculated using GraphPad software, fitting to a single-phase exponential decay equation.

Pharmacokinetics. Compound **6c** was administered to mice i.p. at a dosage of 25 mg/kg. Blood and brain samples were collected at six time points (0, 0.25, 0.5, 1.0, and 2.0 h) from three animals at each time point. For plasma measurements, blood (approximately 250 μl) was collected via retro-orbital puncture into tubes containing sodium heparin anticoagulant. Plasma was separated via centrifugation (4°C, 3500 rpm, 10 min) and stored at -80°C. At the time of measurement, frozen plasma samples were thawed at room temperature and vortexed thoroughly. Plasma (25 μl) was transferred into a 1.5 ml Eppendorf tube. To each sample, 25μl of methanol and 25 μl of the internal standard were added, followed by the addition of 100 μl of methanol. The sample mixture was vortexed for approximately 1 min. After centrifugation at 11,000 g for 5 min, the upper organic layer was transferred to a glass tube and evaporated at 40°C under a gentle stream of nitrogen. Residues were dissolved in 150 μl of the mobile phase and mixed using a Vortex mixer. A 20 μl aliquot of the resulting solution was injected onto the liquid chromatography/ mass spectrometry (LC/MS) Shimadzu system for analysis. For measurement of brain concentrations, mice were killed by cervical dislocation after blood harvest. Brains were immediately excised, weighed, and rinsed by cold saline and then frozen at -80°C until further processing for LC/MS analysis. On the day of the assay, frozen tissue samples were thawed unassisted at room temperature. When completely thawed, each tissue sample of 200 mg was weighed and placed into a plastic tube. Methanol (1.0 ml) was added and homogenization conducted using a pellet pestle cordless motor homogenizer for approximately 1 min. Then, the samples were vortexed for 1 min and a 25 μl aliquot was transferred into an Eppendorf tube. To

each sample, 25 µl of methanol and the samples centrifuged at 11,000 g for 5 min. A 20 µl aliquot of the supernatants was diluted to 60 µl with the mobile phase (H_2O/acetonitrile with 5% formic acid), and a 10 µl aliquot was injected onto the LC/MS system for analysis. Quantification of the drug concentration in each aliquot was achieved by using the standard curve method. Half-life was calculated using GraphPad software, fitting to a single-phase exponential decay equation.

Hippocampal cGMP levels. 2-3 month old male and female mice (20-25 g; C57Bl6 mice) were injected with **6c** (3 mg/kg, 2% DMSO & 2% Tween, i.p.) or Vehicle (2% DMSO & 2% Tween, i.p.). Thirty min after administration of vehicle or **6c**, mice were subjected to foot shock and sacrificed 10 sec, 1 min and 3 min after shock by cervical dislocation and decapitation. The hippocampal samples were extracted and snap frozen in liquid nitrogen. Levels of cGMP were quantitated by Enzyme Immunoassay procedure (Cayman Chemical Company, Item no. 581021) following the manufacturer's guidelines in duplicate. cGMP levels were normalized with the protein concentration calculated using BCA Protein Assay Reagent (Thermo Scientific).

Electrophysiology. Hippocampal slices were cut as previously described[16]. Briefly, 3–4 month old animals were sacrificed and their hippocampi extracted. 400 µ m slices were obtained and maintained in an interface chamber continuously perfused with a solution (ACSF) consisting of (in mM): 124.0 NaCl, 4.4 KCl, 1.0 Na_2HPO_4, 25.0 $NaHCO_3$, 2.0 $CaCl_2$, 2.0 $MgCl_2$, and 10.0 glucose, and bubbled with 95% O_2 and 5% CO_2. Extracellular recordings were performed by stimulating the Schaeffer collateral fibers and recording in CA1 *stratum radiatum* with a glass electrode filled with ACSF. Following recording of a 20 min baseline, LTP was evoked through

a theta-burst stimulation (four pulses at 100 Hz, with the bursts repeated at 5 Hz and each tetanus including three 10-burst trains separated by 15 sec).

Behavioral Studies. Fear conditioning was assessed as previously described[30, 32]. Training for fear conditioning was performed by placing the mouse in a conditioning chamber for 2 min before the onset of a tone (Conditioned Stimulus (CS), 30 sec, 85 dB sound at 2800 Hz). In the last 2 sec of the CS, mice were given a 2 sec, 0.7 mA mild foot shock (Unconditioned Stimulus, (US)) through the bars of the floor. After the US, the mice were left in the chamber for another 30 s. Freezing behavior, defined as the absence of movements except for respiratory excursions, was scored using Freezeview software (Med Associates, St. Albans, VT). Contextual fear learning was evaluated 24 hrs after training by measuring freezing responses for 5 min in the same chamber where the mice were trained. Cued fear learning was evaluated 24 hrs after contextual testing (Supporting Information, Fig. S9). The mice were placed in a novel context for 2 min (pre-CS test), after which they were given a CS for 3 min (CS test), and freezing behavior was measured during the first 30 sec that mimic the CS-US conditioning and the remaining 2.5 min.

The radial arm water maze task, a hybrid of the classic Morris Water Maze and the radial arm land maze, was performed as previously described[39]. The mouse had to swim in 6 alleys (arms) radiating from a central area until it found a hidden (submerged) platform at the end of one of the arms, based on visual cues placed in the room. The first day of the protocol was a training day on which mice were trained to identify the platform location by alternating between a visible and a hidden platform in a goal arm. The final 3 trials on that day and all 15 trials on day 2 used a hidden escape platform to force mice to use spatial cues to identify the location of the goal arm.

To avoid learning limitations imposed by exhausting practice and to avoid fatigue that may result from consecutive trials, spaced practice training was established by running the mice in cohorts of 4 and alternating different cohorts through the 15 training trials over 3-hour testing periods each day. The number of incorrect arm entries (entries to arms with no platform) was counted.

If the animal entered the incorrect arm it was gently pulled back to the start arm. Failure to select an arm after 15 sec was counted as an error and the mouse was returned to the start arm. Each trial lasted up to 1 min. After 1 min, if the platform had not been located, the mouse was guided gently through the water by placing a hand behind it to direct it towards the platform. The mouse rested on the platform for 15 sec. The goal platform location was different for each mouse. On day 2, the same procedure was repeated as on day 1 for all 15 trials using only the hidden platform. For data analysis, averages for each mouse were calculated using blocks of 3 trials.

Behavioral testing included also control tasks. Specifically, evaluation of the visible platform task was performed to exclude motor, sensorial, and motivational defects. Speed and time (latency) to reach the platform was observed among the different groups of mice (Supporting Information, Figure S10).[30]

Statistical Analyses. Experiments were performed in blind. Results were expressed as Standard Error of the Mean (SEM). Level of significance was set for $p<0.05$. Results were analyzed by student t-test/2-way ANOVA for repeated measures. Planned comparisons were used for posthoc analysis.

Animals. The animal protocols for PK studies, measurement of hippocampal cGMP levels, and behavioral assessment were approved by the Columbia University Institutional Animal Care

and Use Committee (IACUC). The animals were maintained on a 12 h light/dark cycle (with light onset at 6:00 A.M.) in temperature and humidity-controlled rooms of the Columbia University Animal Facility. Food and water were available ad libitum.

ASSOCIATED CONTENT

Supporting Information.

The Supporting Information is available free of charge via the Internet at http://pubs.acs.org.

^{1}H-NMR and 1D NOESY spectra of compound **5c** and **6c**, PDE5 cGMP pocket in available crystal structures, compounds **6c** and **24a** superposed in their two docking poses, interaction diagrams for compound **24a** docking poses, predicted binding free energies for compounds in the Naphthydrine and 1*H*-pyrroloquinolinone series, cued learning test and visible platform and speed tests for compound **6c** (PDF)

SMILES strings and IC_{50} data for compounds **6a-g**, **14**, **17a-d**, and **24a-f** (CSV)

AUTHOR INFORMATION

Corresponding Authors

*For D.W.L.: phone: +1 212 305 5838; Email: dwl1@columbia.edu

*For O.A.: phone: +1 212 342 0533; Email: oa1@columbia.edu

Present Addresses

†For J.V.: Schrödinger Inc., 120 West 45th Street, 17th Floor, New York, NY 10036

[†]For F.S.: Department of Pathology, New York Medical College at Westchester Medical Center, 100 Woods Rd - Macy Pavilion, Valhalla, NY 10595

[†]For S.Y.: Department of Pharmacology & Toxicology and Higuchi Bioscience Center, School of Pharmacy, University of Kansas, Lawrence, KS 66047

Author Contributions

[#]J.F. and J.V. contributed equally. All authors have given approval to the final version of the manuscript.

ACKNOWLEDGMENT

This work was supported by the National Institute of Aging at the National Institutes of Health, grant number U01-AG032973, the National Institutes if Health grant number 1S10OD018121-01, and the National Center for Advancing Translational Sciences, National Institutes of Health, through Grant Number UL1TR000040. The content is solely the responsibility of the authors and does not necessarily represent the official views of the NIH. The authors gratefully thank Dr. Yitshak. I. Francis, Sudha Rao, and Devarshi M. Thakkar for helping with the cGMP ELISA experiment.

ABBREVIATIONS

NO, Nitric Oxide; sGC, soluble Guanylyl Cyclase; PKG, Protein Kinase G; CREB, cAMP response element binding protein; PS1, Preseniline 1; ACE-Cl, α-chloroethyl chloroformate; TEA, Triethylamine; DIAD, Diisopropyl azodicarboxylate; DIPEA, *N*,*N*-Diisopropylethylamine; tPSA, Topological Polar Surface Area; HLM, Human Liver Microsomes; MLM, Mouse Liver Microsomes; RAWM, Radial Arm Water Maze; FC, Fear Conditioning; NOESY, Steady-state and Transient NOE.

REFERENCES

1. Anand, R.; Gill, K. D.; Mahdi, A. A. Therapeutics of Alzheimer's disease: Past, present and future. *Neuropharmacology* **2014,** *76 Pt A*, 27-50.

2. Cummings, J. L.; Morstorf, T.; Zhong, K. Alzheimer's disease drug-development pipeline: few candidates, frequent failures. *Alzheimer's Res. Ther.* **2014,** *6*, 37.

3. Doody, R. S.; Thomas, R. G.; Farlow, M.; Iwatsubo, T.; Vellas, B.; Joffe, S.; Kieburtz, K.; Raman, R.; Sun, X.; Aisen, P. S.; Siemers, E.; Liu-Seifert, H.; Mohs, R.; Alzheimer's Disease Cooperative Study Steering Committee; Solanezumab Study Group. Phase 3 trials of solanezumab for mild-to-moderate Alzheimer's disease. *N. Engl. J. Med.* **2014,** *370*, 311-321.

4. Salloway, S.; Sperling, R.; Fox, N. C.; Blennow, K.; Klunk, W.; Raskind, M.; Sabbagh, M.; Honig, L. S.; Porsteinsson, A. P.; Ferris, S.; Reichert, M.; Ketter, N.; Nejadnik, B.; Guenzler, V.; Miloslavsky, M.; Wang, D.; Lu, Y.; Lull, J.; Tudor, I. C.; Liu, E.; Grundman, M.; Yuen, E.; Black, R.; Brashear, H. R.; Bapineuzumab 301 and 302 Clinical Trial Investigators. Two phase 3 trials of bapineuzumab in mild-to-moderate Alzheimer's disease. *N. Engl. J. Med.* **2014,** *370*, 322-333.

5. Sevigny, J.; Chiao, P.; Bussiere, T.; Weinreb, P. H.; Williams, L.; Maier, M.; Dunstan, R.; Salloway, S.; Chen, T.; Ling, Y.; O'Gorman, J.; Qian, F.; Arastu, M.; Li, M.; Chollate, S.; Brennan, M. S.; Quintero-Monzon, O.; Scannevin, R. H.; Arnold, H. M.; Engber, T.; Rhodes, K.; Ferrero, J.; Hang, Y.; Mikulskis, A.; Grimm, J.; Hock, C.; Nitsch, R. M.; Sandrock, A. The antibody aducanumab reduces Abeta plaques in Alzheimer's disease. *Nature* **2016,** *537*, 50-56.

6. Puzzo, D.; Palmeri, A.; Arancio, O. Involvement of the nitric oxide pathway in synaptic dysfunction following amyloid elevation in Alzheimer's disease. *Rev. Neurosci.* **2006,** *17*, 497-523.

7. Lu, Y. F.; Kandel, E. R.; Hawkins, R. D. Nitric oxide signaling contributes to late-phase LTP and CREB phosphorylation in the hippocampus. *J. Neurosci.* **1999,** *19*, 10250-10261.

8. Wong, J. C.; Bathina, M.; Fiscus, R. R. Cyclic GMP/protein kinase G type-Ialpha (PKG-Ialpha) signaling pathway promotes CREB phosphorylation and maintains higher c-IAP1, livin, survivin, and Mcl-1 expression and the inhibition of PKG-Ialpha kinase activity synergizes with cisplatin in non-small cell lung cancer cells. *J. Cell. Biochem.* **2012,** *113*, 3587-3598.

9. Silva, A. J.; Kogan, J. H.; Frankland, P. W.; Kida, S. CREB and memory. *Annu. Rev. Neurosci.* **1998,** *21*, 127-148.

10. Barco, A.; Alarcon, J. M.; Kandel, E. R. Expression of constitutively active CREB protein facilitates the late phase of long-term potentiation by enhancing synaptic capture. *Cell* **2002,** *108*, 689-703.

11. Benito, E.; Barco, A. CREB's control of intrinsic and synaptic plasticity: implications for CREB-dependent memory models. *Trends Neurosci.* **2010,** *33*, 230-240.

12. Bender, A. T.; Beavo, J. A. Cyclic nucleotide phosphodiesterases: molecular regulation to clinical use. *Pharmacol. Rev.* **2006,** *58*, 488-520.

13. Maurice, D. H.; Ke, H.; Ahmad, F.; Wang, Y.; Chung, J.; Manganiello, V. C. Advances in targeting cyclic nucleotide phosphodiesterases. *Nat. Rev. Drug Discovery* **2014,** *13*, 290-314.

14. Heckman, P. R.; Wouters, C.; Prickaerts, J. Phosphodiesterase inhibitors as a target for cognition enhancement in aging and Alzheimer's disease: a translational overview. *Curr. Pharm. Des.* **2014,** *21*, 317-331.

15. Garcia-Osta, A.; Cuadrado-Tejedor, M.; Garcia-Barroso, C.; Oyarzabal, J.; Franco, R. Phosphodiesterases as therapeutic targets for Alzheimer's disease. *ACS Chem. Neurosci.* **2012,** *3*, 832-844.

16. Puzzo, D.; Vitolo, O.; Trinchese, F.; Jacob, J. P.; Palmeri, A.; Arancio, O. Amyloid-beta peptide inhibits activation of the nitric oxide/cGMP/cAMP-responsive element-binding protein pathway during hippocampal synaptic plasticity. *J. Neurosci.* **2005,** *25*, 6887-6897.

17. Puzzo, D.; Staniszewski, A.; Deng, S. X.; Privitera, L.; Leznik, E.; Liu, S.; Zhang, H.; Feng, Y.; Palmeri, A.; Landry, D. W.; Arancio, O. Phosphodiesterase 5 inhibition improves synaptic function, memory, and amyloid-beta load in an Alzheimer's disease mouse model. *J. Neurosci.* **2009,** *29*, 8075-8086.

18. Fiorito, J.; Saeed, F.; Zhang, H.; Staniszewski, A.; Feng, Y.; Francis, Y. I.; Rao, S.; Thakkar, D. M.; Deng, S. X.; Landry, D. W.; Arancio, O. Synthesis of quinoline derivatives: discovery of a potent and selective phosphodiesterase 5 inhibitor for the treatment of Alzheimer's disease. *Eur. J. Med. Chem.* **2013,** *60*, 285-294.

19. Puzzo, D.; Lee, L.; Palmeri, A.; Calabrese, G.; Arancio, O. Behavioral assays with mouse models of Alzheimer's disease: practical considerations and guidelines. *Biochem. Pharmacol.* **2014,** *88*, 450-467.

20. Wang, L.; Wu, Y.; Deng, Y.; Kim, B.; Pierce, L.; Krilov, G.; Lupyan, D.; Robinson, S.; Dahlgren, M. K.; Greenwood, J.; Romero, D. L.; Masse, C.; Knight, J. L.; Steinbrecher, T.; Beuming, T.; Damm, W.; Harder, E.; Sherman, W.; Brewer, M.; Wester, R.; Murcko, M.; Frye, L.; Farid, R.; Lin, T.; Mobley, D. L.; Jorgensen, W. L.; Berne, B. J.; Friesner, R. A.; Abel, R. Accurate and reliable prediction of relative ligand binding potency in prospective drug discovery by way of a modern free-energy calculation protocol and force field. *J. Am. Chem. Soc.* **2015,** *137*, 2695-2703.

21. Zwanzig, R. W. High-temperature equation of state by a perturbation method. I. Nonpolar gases. *J. Chem. Phys.* **1954,** *22*, 1420-1426.

22. Snieckus, V. A. O., T.; Boekelheide, V. Stereoselective syntheses of isoquinuclidones. I. *J. Org. Chem.* **1972,** *37* 2845-2848.

23. Wolinska, E. P., Ekaterina; Strekowski, Lucjan Facile synthesis of 1,2,3,4-tetrahydrobenzo[b][1,6]naphthyridines. *Heterocycl. Commun.* **2009,** *15*, 63-65.

24. Hu, D. X.; Grice, P.; Ley, S. V. Rotamers or diastereomers? An overlooked NMR solution. *J. Org. Chem.* **2012,** *77*, 5198-5202.

25. Cote, R. H. Characteristics of photoreceptor PDE (PDE6): similarities and differences to PDE5. *Int. J. Impotence Res.* **2004,** *16 Suppl 1*, S28-33.

26. Abel, R.; Young, T.; Farid, R.; Berne, B. J.; Friesner, R. A. Role of the active-site solvent in the thermodynamics of factor Xa ligand binding. *J. Am. Chem. Soc.* **2008,** *130*, 2817-2831.

27. Young, T.; Abel, R.; Kim, B.; Berne, B. J.; Friesner, R. A. Motifs for molecular recognition exploiting hydrophobic enclosure in protein-ligand binding. *Proc. Natl. Acad. Sci. U. S. A.* **2007,** *104*, 808-813.

28. Hitchcock, S. A.; Pennington, L. D. Structure-brain exposure relationships. *J. Med. Chem.* **2006,** *49*, 7559-7583.

29. Rowan, M. J.; Klyubin, I.; Cullen, W. K.; Anwyl, R. Synaptic plasticity in animal models of early Alzheimer's disease. *Philos. Trans. R. Soc., B* **2003,** *358*, 821-828.

30. Trinchese, F.; Liu, S.; Battaglia, F.; Walter, S.; Mathews, P. M.; Arancio, O. Progressive age-related development of Alzheimer-like pathology in APP/PS1 mice. *Ann. Neurol.* **2004,** *55*, 801-814.

31. Mensch, J.; Oyarzabal, J.; Mackie, C.; Augustijns, P. In vivo, in vitro and in silico methods for small molecule transfer across the BBB. *J. Pharm. Sci.* **2009,** *98*, 4429-4468.

32. Gong, B.; Vitolo, O. V.; Trinchese, F.; Liu, S.; Shelanski, M.; Arancio, O. Persistent improvement in synaptic and cognitive functions in an Alzheimer mouse model after rolipram treatment. *J. Clin. Invest.* **2004,** *114*, 1624-1634.

33. Hughes, R. O.; Maddux, T.; Joseph Rogier, D.; Lu, S.; Walker, J. K.; Jon Jacobsen, E.; Rumsey, J. M.; Zheng, Y.; Macinnes, A.; Bond, B. R.; Han, S. Investigation of the pyrazinones as PDE5 inhibitors: evaluation of regioisomeric projections into the solvent region. *Bioorg. Med. Chem. Lett.* **2011,** *21*, 6348-6352.

34. Sastry, G. M.; Adzhigirey, M.; Day, T.; Annabhimoju, R.; Sherman, W. Protein and ligand preparation: parameters, protocols, and influence on virtual screening enrichments. *J. Comput.-Aided Mol. Des.* **2013,** *27*, 221-234.

35. Halgren, T. A.; Murphy, R. B.; Friesner, R. A.; Beard, H. S.; Frye, L. L.; Pollard, W. T.; Banks, J. L. Glide: a new approach for rapid, accurate docking and scoring. 2. Enrichment factors in database screening. *J. Med. Chem.* **2004,** *47*, 1750-1759.

36. Friesner, R. A.; Banks, J. L.; Murphy, R. B.; Halgren, T. A.; Klicic, J. J.; Mainz, D. T.; Repasky, M. P.; Knoll, E. H.; Shelley, M.; Perry, J. K.; Shaw, D. E.; Francis, P.; Shenkin, P. S. Glide: a new approach for rapid, accurate docking and scoring. 1. Method and assessment of docking accuracy. *J. Med. Chem.* **2004,** *47*, 1739-1749.

37. Lazaridis, T. Inhomogeneous fluid approach to solvation thermodynamics. 1. Theory. *J. Phys. Chem. B* **1998,** *102*, 3531–3541.

38. Lazaridis, T. Inhomogeneous fluid approach to solvation thermodynamics. 2. Applications to simple fluids. *J. Phys. Chem. B* **1998,** *102*, 3542–3550.

39. Alamed, J.; Wilcock, D. M.; Diamond, D. M.; Gordon, M. N.; Morgan, D. Two-day radial-arm water maze learning and memory task; robust resolution of amyloid-related memory deficits in transgenic mice. *Nat. Protoc.* **2006,** *1*, 1671-1679.

Table of Contents Graphic